

Radiation Physics and Chemistry

Observation of Self-Healing and Blue Response Enhancement in c-Si Solar Cells Exposed to Electron Irradiation

--Manuscript Draft--

Manuscript Number:	RPC-D-24-01859R1
Article Type:	Full Length Article
Section/Category:	Radiation Physics
Keywords:	Solar cell; Electron irradiation; Aged c-Si solar cell; Electrical characterization; Self-healing effect
Abstract:	The effects of electron irradiation on the performance of mono-crystalline silicon (c-Si) solar cells were investigated by examining various electron doses, ranging from 225 to 900 Gy, with an energy of 8 MeV. The study focused on dose-dependent degradation in cell behavior resulting from irradiation. Detailed analysis was conducted through dark and illuminated current-voltage (I-V) measurements, external quantum efficiency (EQE) measurements, capacitance-voltage (C-V) measurements, and conductance-voltage (G/ ω -V) measurements. The observed degradations were thoroughly analyzed, quantified, and discussed by comparing the results obtained from complementary electrical and optical characterizations of the cells before and after irradiation. The experimental findings indicated that the degradation in cell parameters was attributed to irradiation-induced defect formations in the base layer. However, the devices were found to be resilient to defect formations in the emitter and near the depletion edge of the base. After 52 months of irradiation, significant self-healing effects and improvements in blue response were observed in the cells, likely due to additional positive charge formation in the nitride layer from oxynitride formation in the ambient atmosphere over time, accelerated by radiation damage. This was confirmed by both illuminated I-V and EQE measurements.

REBUTTAL LETTER

Manuscript ID: RPC-D-24-01859

Reviewer: 2

We thank the referee for objective criticism of our work. We did take into consideration the comments and provide our responses below along with modifications to the manuscript.

Comments:

The study investigates the effects of electron irradiation on mono-crystalline silicon (c-Si) solar cells by analyzing dose-dependent degradation using a range of characterization techniques, including I-V, EQE, C-V, and G/ ω -V measurements. The findings reveal that irradiation-induced defects in the base layer cause performance degradation, while the emitter and depletion edge show resilience to defect formation. Notably, significant self-healing effects and improved blue response are observed after prolonged irradiation, attributed to positive charge accumulation in the nitride layer from oxynitride formation. This work provides valuable insights into the mechanisms of radiation-induced degradation and recovery in c-Si solar cells.

While the results are intriguing, some corrections are necessary for publication, such as providing greater clarity on experimental methodologies, addressing ambiguities in the analysis of defect dynamics, and ensuring more detailed discussions of self-healing mechanisms and their reproducibility. Once these issues are addressed, the work will be a strong contribution to the field of semiconductor device reliability under radiation exposure.

C1) Line 7, the percentage should be after the figure, this error is also noticed all through the manuscript, hence the entire manuscript has to be checked to correct the mistake

A1) Corrected in the text.

C2) There are few grammatical errors that needs to be corrected, for example, line 55 “it is critical to understand the behavior of the cells that exposed to that are exposed instead of that exposed.

A2) Corrected in the text.

C3) There is also an error due to grammar in line 27 of Pg 3. “are” is missing before well understood.

A3) Corrected in the text.

- C4)** References about radiation studies on Si-based devices of different particle type, fluence and energy should be included. These articles can be used to report on these studies
1. Electrical properties of 3 MeV proton irradiated silicon Schottky diodes. *Physica B: Condensed Matter* 610 (2021): 412786.
 2. Current-voltage characteristics of 4 MeV proton-irradiated silicon diodes at room temperature. *Silicon*, 14(16) (2022), 10237-10244.
 3. Suppression of irradiation effect on electrical properties of silicon diodes by iron in psilicon." *Radiation Effects and Defects in Solids* (2024): 1-14.
 4. Enhancing Radiation-Hardness of Si-based Diodes: An Investigation of Al-Doping Effects in Si Using IV Measurements. *Radiation Physics and Chemistry* (2024): 111873.

A4) Dependent on the suggestions by our referee we put these suggested references into the text.

C5) Line 53, unirradiated reads better than unexposed in this context.

A5) Corrected in the text.

C6) The schematic or pictorial depiction of the fabricated cells should be provided in this section.

A6) Schematic of the fabricated cells added to the materials and methods section.

C7) The voltage range for the I-V, C-V and G/w-V measurement should be provided with the reason for the chosen range given

A7) The voltage range for I-V curves given for -2 to + 0.75 V range are given: As the device is Si cell, we considered given range sufficient to allow observation of irradiation effects on Si cell within its operation range.

C-V and G-V measurements are done with a frequency range of 1 to 100 kHz, however for all frequencies there was no change in the results by changing frequency. This could be due to the screening effect by dominancy of edge effect (due to degradation by laser cut). Therefore only 100 kHz results are put into the manuscript. In C-V the voltage range is chosen to capture the transition from full depletion to partial depletion and to see the start point of bulk transport dominancy over junction effect (the point where C-V curve makes peak in forward bias regime). The range is sufficient to provide meaningful insights into the bulk and interface states of the cells. G-V results extended to +5 V to try to see the effects of irradiation on the bulk transport behaviour of the cells beyond the depletion region.

C8) Authors should also give reason why the chosen electron doses were used (225, 450, 675 and 900)

A8) In accordance with the permission obtained from the facility, this study was planned with durations of 0.5, 1, 1.5, and 2 hours, with dose amounts corresponding to these time periods.

C9) It would have been more interesting to have data for more months interval, for example 12, 24, 36, 48, 60 months, this data would have given more information of how the cell performs over time.

A9) We appreciate the reviewer's suggestion to include data at more frequent intervals over time. The initial experiment was designed to investigate the effects of electron dose on solar cells, rather than their performance over extended time intervals. However, after 52 months, the same measurements were repeated to examine the state of the irradiated samples just to see possible changes over time. While this provided additional insights, the study did not include a systematically planned investigation as suggested. We acknowledge the value of such a study and agree that future research could be specifically designed to include data from longer time intervals, such as 12, 24, 36, 48, and 60 months, to provide a more detailed understanding of the long-term performance of solar cells.

C10) The first sentence is too long and boring, it should be revised for easy understanding.

A10) The sentence “Room temperature dark I-V measurement results of solar cells before, just after and after 52 months of irradiation for different electron doses are shown comparatively in Fig. 1 and diode ideality factors calculated by using single diode model from these curves are given in Table 1.” is replaced in the manuscript with new sentences “Room temperature dark I-V measurement results of solar cells before, just after and after 52 months of irradiation for different electron doses are shown comparatively in Fig. 2. Diode ideality factors calculated by using single diode model from these curves are given in Table 1.”

C11) The statement “diode ideality factor goes to increase which indication of creation of generation-recombination level within the band gap of Si” is full of grammatical error rendering the sentence meaningless. I want to believe the authors are trying to explain the increase in the value of ideality factor after irradiation which may be attributed to the generation-recombination centers introduced by the irradiation-induced defects.

A11) The sentence “As seen in the table, with the increase in radiation dose, diode ideality factor goes to increase which indication of creation of generation-recombination levels within the bandgap of Si.” is replaced in the manuscript with new sentences “As observed in the table, with the radiation dose increases, the diode ideality factor also increases, suggesting the formation of generation-recombination (G-R) levels by the irradiation-induced defects within the bandgap of Si, which impacts the diode's electrical behavior.”

C12) I suggest the results in figure 1 can be presented in a simpler form that will aid easy comparison and understanding. Two plots (a and b) for before and after irradiation with every dose plotted a single plot.

A12) The reviewer comment totally right. However, the samples used in the study were derived from a full wafer cell by laser-cutting into smaller cells of equal area. However, the electrical behaviors of these cells is not entirely identical and shows some variations. Therefore, while creating the graphs, we analyzed the changes within each sample individually and presented

the results in separate plots for clarity and accuracy. Combining the data into a single plot might obscure these sample-specific variations.

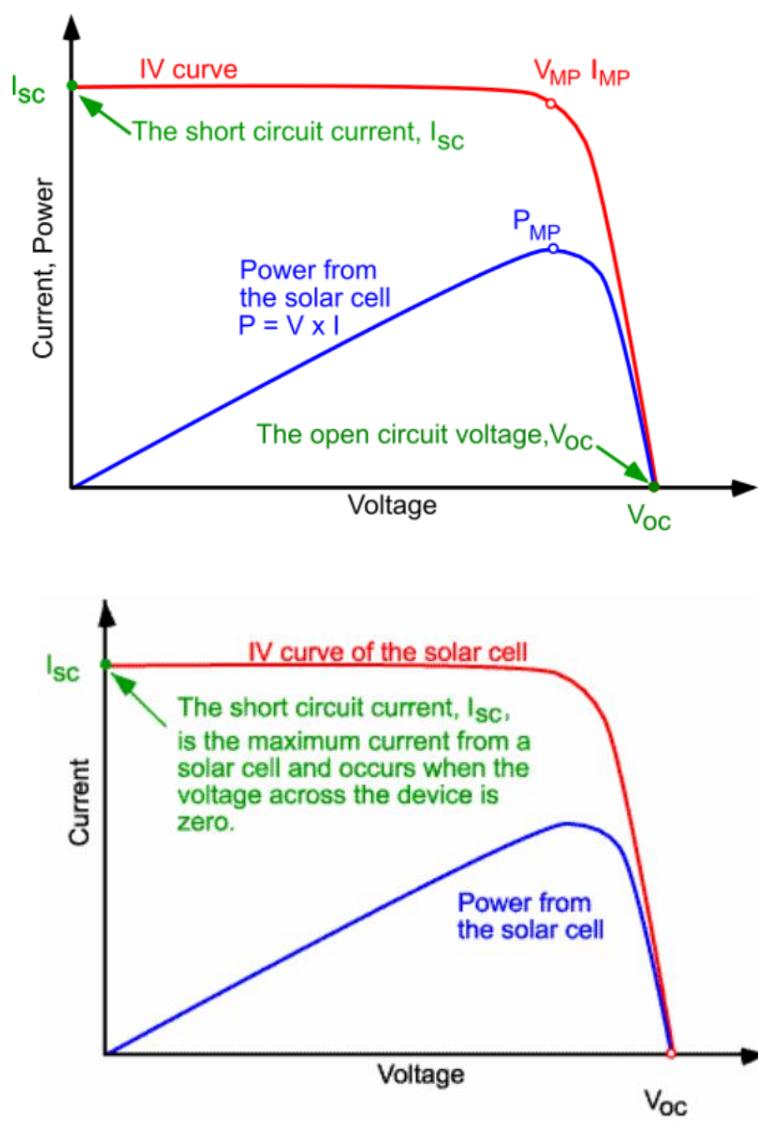
C13) The parameters evaluated for the cells needs to be explained in a better way most especially how they are obtained.

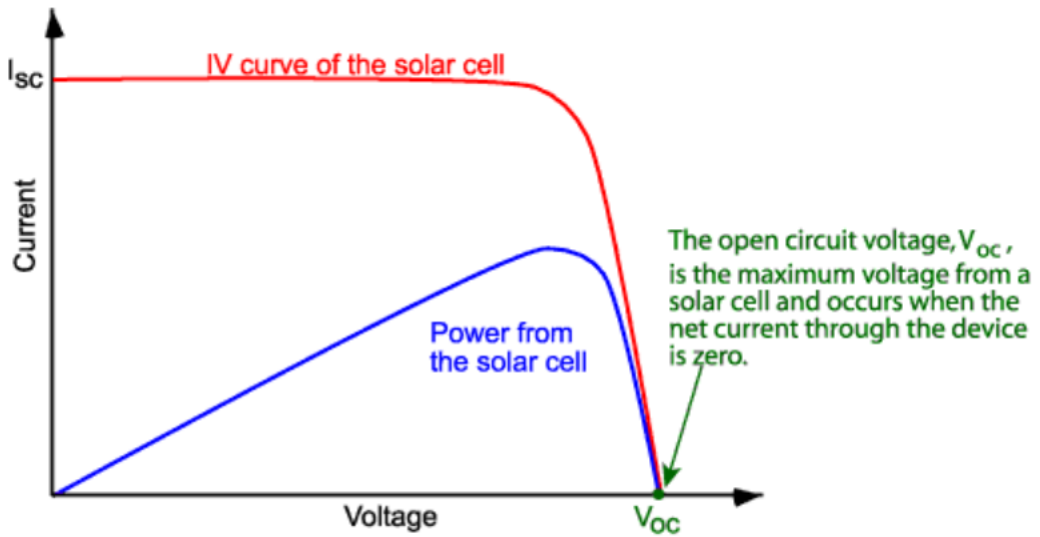
A13) I-V characteristics of Si solar cells under illumination were measured at room temperature using a Keithley 2440 Source meter. The cells were illuminated under AM1.5G condition using an Abet 2000 solar simulator with illumination intensity set to 1000 W.m^{-2} .

The figures given below are taken from <https://www.pveducation.org/pvcdrom/welcome-to-pvcdrom> web page.

The determination of solar cell parameters is presented using the graphs and formulas below.

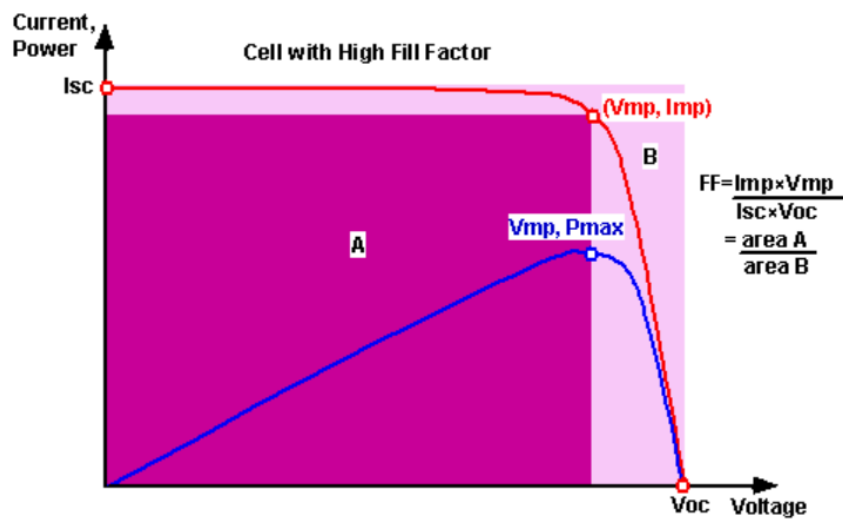
The positions of I_{sc} and V_{oc} on the I-V curve of the solar cell are shown in the graph below.





The fill factor (FF) can be expressed as,

$$FF = \frac{V_{mp} I_{mp}}{V_{oc} I_{sc}}$$



The conversion efficiency (η) of light into electric power, for a solar cell is given by

$$P_{max} = V_{oc} I_{sc} FF$$

$$\eta = \frac{V_{oc} I_{sc} FF}{P_{in}}$$

The R_s of a solar cell can be determined from its I-V curve using the formula as follows. This involves analyzing the slope of the I-V curve near the V_{oc} , which is the voltage at zero current.

$$R_s = -\frac{dV}{dI} \Big|_{V \approx V_{oc}}$$

The R_{sh} of a solar cell can be determined from its I-V curve using the formula as follows. This involves analyzing the slope of the I-V curve near the I_{sc} , which is the current at zero voltage.

$$R_{sh} = -\frac{dV}{dI} \Big|_{I \approx I_{sc}}$$

C14) The caption for the figures needs to be rephrased to enhance simplicity and better understanding.

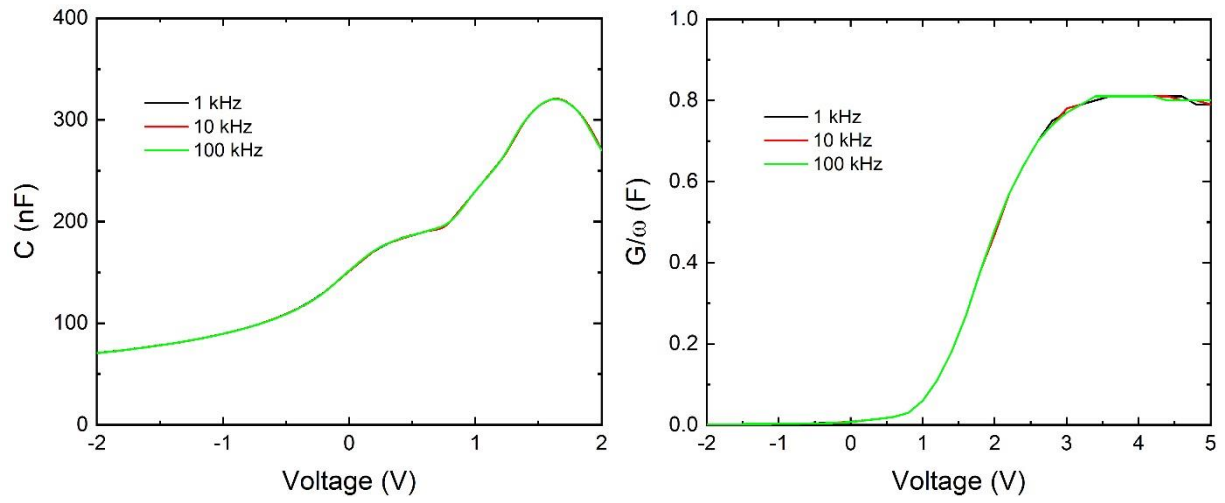
A14) Under the suggestions of the reviewer, the caption of the figures rephrased in the manuscript.

C15) The parameters provided in Figure 3 are not well defined anywhere in the manuscript.

A15) Figure 3 becomes Figure 4 in revised manuscript. How parameters calculated and their descriptions are clarified in manuscript.

C16) The C-V and G/w-V measurements were taken at a frequency of 100 kHz, however, the reason for choosing this frequency was not provided and it is very imperative.

A16) Actually measurements were taken between 1 kHz to 100 kHz frequency range. However, any change has been observed in the curves of different frequency. Below C-V and G-V measurement results one of the unirradiated cells is given for 1 kHz, 10 kHz and 100 kHz. The lack of significant variation between 1 kHz and 100 kHz suggests that the dominant processes are fast and not limited by carrier trapping or slow defect dynamics. Which may be due to the edges of the cells. When cells cut from a full wafer cell, the edges of the cells degraded, and metal residues or metal/Si phases may form around the edge. Which could screen the response of the defects with respect to frequency change under overall response of the cells.



C17) There is a peak observed in the forward bias of the C-V characteristics and there is no explanation given about the observed peaks.

A17) We thank to our referee for this comment. The explanations has been added into the manuscript.

REBUTTAL LETTER

Manuscript ID: RPC-D-24-01859

Reviewer: 3

We thank the referee for objective criticism of our work. We did take into consideration the comments and provide our responses below along with modifications to the manuscript.

Comments:

The paper presents valuable findings on the effects of electron irradiation on c-Si solar cells, contributing to the understanding of their performance in radiation-rich environments. However, addressing the identified weaknesses could significantly improve the quality and impact of the research by providing a more detailed and comprehensive analysis of the findings.

As a reviewer of this paper, I would like to provide the following detailed comments, emphasizing both the strengths and weaknesses of the study.

Strengths:

1. Comprehensive Analysis: The paper presents a thorough investigation of dose-dependent degradation in solar cell performance due to irradiation. The use of various characterization techniques, such as dark and illuminated current-voltage (I-V) measurements, external quantum efficiency (EQE) measurements, capacitance-voltage (C-V) measurements, and conductance-voltage (G/ ω -V) measurements, offers a well-rounded understanding of the irradiation effects on the performance of the solar cells.
2. Insight into Self-Healing Mechanisms: The observation of significant self-healing effects, including improvements in blue response after 52 months of irradiation, is a notable finding. This insight into the resilience of c-Si solar cells under prolonged radiation exposure is valuable for future applications, especially in space or high-radiation environments, where long-term performance is critical.
3. Relevance to Solar Cell Technology: The study addresses a crucial aspect of solar cell technology, particularly for applications in environments where radiation exposure is a concern. The findings could inform the design of more robust solar cells, enhancing their longevity and efficiency in extreme conditions.

C1) Limited Discussion on Mechanisms: While the paper identifies defect formation in the base layer as a cause of degradation, it would benefit from a more detailed discussion on the underlying mechanisms of defect formation and their impact on overall solar cell performance. A deeper exploration of the physical and chemical processes involved would provide a more comprehensive understanding of the degradation mechanisms.

Add a section that explains in detail the mechanisms leading to defect formation and how they affect the performance of solar cells.

A1) We extend our gratitude to the reviewer for their valuable feedback.

Possible types of defects have been added into the introduction section in the manuscript through a comprehensive literature review.

C2) Lack of Comparative Analysis: The study primarily focuses on c-Si solar cells without making comparisons to other types of solar cells (e.g., thin-film or multi-junction cells). Including such comparisons could provide a broader context for the findings and highlight the unique advantages or limitations of c-Si technology in radiation environments.

Include a comparative analysis with other solar cell types to provide a broader context regarding the effectiveness of monocrystalline silicon cells in radiation environments.

A2) We appreciate the reviewer's comment pointing out the importance of comparative analysis. We agree that providing a broader context by comparing the results with other solar cell technologies could enhance the understanding of the effectiveness of monocrystalline silicon (c-Si) cells in radiation environments. This comparative analysis has been added to the introduction section of the revised manuscript to provide broader context for the study findings and to underline the unique position of c-Si solar cells in radiation environments.

C3) Figures and Visuals: Although several figures are referenced in the paper, the quality and clarity of these visuals could be improved. Ensuring that figures are well-labeled, with clear legends and easy-to-interpret data, would enhance the overall presentation and readability of the results.

Ensure that all figures and illustrations are clear and informative, with accurate labeling.

A3) We appreciate the reviewer's comments regarding the figures and visuals. Based on the reviewer's feedback, the necessary revisions have been made to the figures and are reflected in the manuscript.

C4) Lack of Information on Environmental Conditions: The environmental conditions under which the experiments were conducted are not adequately detailed. It is important to clarify the temperature, humidity, and pressure, as these factors can influence the experimental results.

Add details about the environmental conditions under which the experiments were conducted, helping to understand the impact of these factors on the results.

A4) We appreciate the reviewer's comments.

All measurements were carried out at room temperature under atmospheric conditions. The air pressure is around 0.92 atm and the humidity is around on average 45%-50%. And the environmental conditions have been added to the manuscript.

REBUTTAL LETTER

Manuscript ID: RPC-D-24-01859

Reviewer: 1

We thank the referee for objective criticism of our work. We did take into consideration the comments and provide our responses below along with modifications to the manuscript.

Comments:

Thank you for your opportunity to review this manuscript. The reviewed manuscript "***Observation of Self-Healing and Blue Response Enhancement in c-Si Solar Cells Exposed to Electron Irradiation***" had reviewed the background and also the latest literatures. I recommend this manuscript after some minor revisions:

C1) In general, solar cells for space application are tested under conditions based on the environment of a satellite in a geostationary orbit (GEO) (at a distance of ~ 36000 km) or low earth orbit (LEO) (at a distance of ~ 500 – 2000 km): 1 MeV electron irradiation with fluence $10^{13} – 10^{16}$ e/cm². Why in this study was chosen as the electron irradiation 8 MeV with a fluence of $1.6 \cdot 10^{11}$ cm⁻²?

A1) We appreciate reviewer comments. Firstly, we realized that the fluence level in the manuscript mistakenly calculated of 1.6×10^{11} cm⁻², the fluence is recalculated and corrected. Recalculated fluences of 225, 450, 675 and 900 Gy corresponding to 1.8×10^{14} to 7.2×10^{14} cm⁻² for the lowest and highest irradiation levels respectively. The correction was done on the manuscript also in the experimental section.

The reviewer totally right about energy of the electron irradiation standards which is mostly done using 1 MeV. While the typical range for space applications lies up to 10 MeV, our decision was made to study a distinct energy level (8 MeV) to investigate the potential effects of this energy on the solar cell's performance, with the goal of contributing new insights to the understanding of radiation impacts across a broader range of energies. We believe this approach provides valuable data for potential applications in various space environments and radiation levels. Moreover, using 8 MeV electrons allows us to also bulk related effects deep inside the device more comprehensively compared to 1 MeV whose damage limited to the near surface regions compared to 8 MeV case.

C2) In section 2 (on page 6, line from 26 to 33), electron beam conditions are described. However, there is no information about the uniformity of the beam. Please mention about beam size and its uniformity, also temperature of Si solar cell during the irradiation.

A2) In an area of 20×20 cm² the electron beam is uniform. Irradiation was done at room temperature, and we did not measure temperature rise in the cells during irradiation. Depending

on the Ref, we expect that the maximum temperature of the cells during the irradiations below 30 °C (Arjhangmehr and Feghhi, 2014).

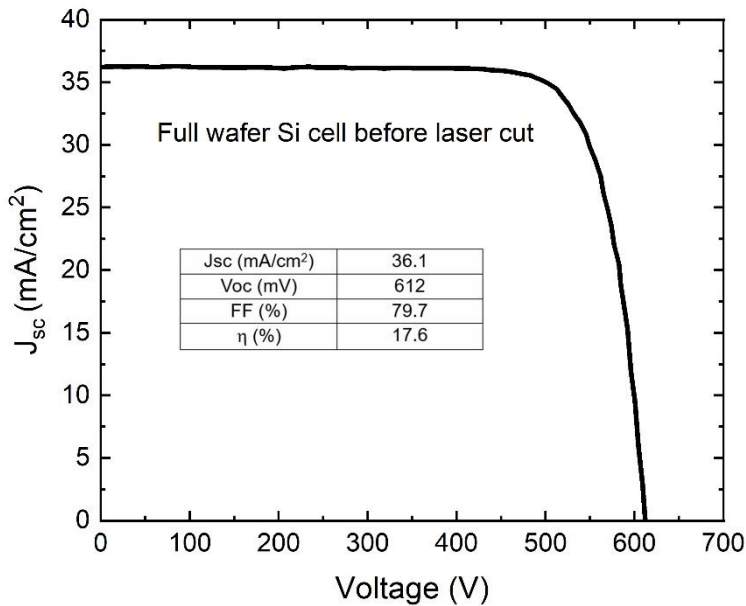
Arjhangmehr, A., Feghhi, S.A.H., 2014. Displacement damage analysis and modified electrical equivalent circuit for electron and photon-irradiated silicon solar cells. *Radiation Effects and Defects in Solids* 169, 874–884.
<https://doi.org/10.1080/10420150.2014.958743>

C3) In section 3 "Results and discussions" given information about the illuminated I-V characteristics of Si solar cells under AM1.5G condition before and after electron irradiation. However, there is no information about the light J-V characteristics under AM0 condition, because light J-V characteristics were conducted under AM0 condition for space use.

A3) Since we do not have the AM0 filter to directly measure the light J-V characteristics under AM0 conditions for space applications, we conducted measurements under AM1.5G conditions instead. Although the AM1.5G spectrum is not identical to AM0, it is widely used for terrestrial applications and provides a good approximation for relative performance. By analyzing the J-V characteristics under AM1.5G, we were able to observe the general behavior of the solar cell and extrapolate its potential performance under AM0 conditions. This relative comparison allows us to gain insights into how the cell might perform in space, despite the lack of direct AM0 measurements.

C4) It would be better if could give graphs of the light J-V characteristics of Si solar cell before and after laser cutting under AM0 condition, since after cutting a solar cell with an area of 15.6 x 15.6 cm² into small area of 2.8 cm² to conduct investigation, efficiency of solar cell decreases due to damage of cell edges. Also, could you give the information on temperature during laser cutting and leakage current after laser cutting?

A4) Since we do not have the AM0 filter to directly measure the light J-V characteristics under AM0 conditions for space applications, we conducted measurements under AM1.5G conditions instead. Although the AM1.5G spectrum is not identical to AM0, it is widely used for terrestrial applications and provides a good approximation for relative performance. Therefore, we could give the full wafer cell I-V curve under AM1.G given below. As reviewer said after laser cut the efficiency off small size cells degraded compared to the un-cut large area cell. The laser cut was done at room temperature; however, we have no idea about the cell temperature exactly during cut. The temperature at the laser spot strike could reach a few thousand °C, however we have no knowledge about exact value. We did not measure dark I-V of full wafer size cell before cutting, however depending on similar cells fabricated that time, we just guess the leakage current could about 1×10^{-6} - 3×10^{-6} A/cm² at about -0.75, -1 V. After laser cut this current increased to 0.5×10^{-5} – 1×10^{-5} A/cm² varying cell to cell.



C5) It is not clear why the FF value does not change after electron irradiation (Fig. 3a). It is known that FF depends on the series and shunt resistance of the solar cell. Usually, the value of series resistance changes after radiation, which is shown in Fig. 4.

A5) Figure 4 becomes Figure 5 in revised manuscript. Thanks to the reviewer for his comment on FF value after irradiation. The series resistance after irradiation tends to change with irradiation as depicted in Figure 5. The observation that the FF value remains unchanged, despite the expectation of changes in series resistance due to radiation, is indeed intriguing. In our study, the unchanged FF value can be attributed to a balance between the competing effects of series and shunt resistances. The unirradiated cells were measured after laser cut on the same day, however irradiation was done at another city and measurements done on the cells after 1 day of irradiation (the situation refers to just after irradiation). Three days pass between laser cut and measurement done on irradiated cells. During these three days there might be changes on the surface of the laser cut edges and irradiation could boost these changes (possibility of metal deposition (Al, Ag) and oxidation etc. On the edge surface).

Almost similar behavior is also observed in Ref (Bhat et al., 2014) where electrons with 8 MeV energy and the used fluence is much higher used in this study.

Bhat, P.S., Rao, A., Krishnan, S., Sanjeev, G., Puthanveettil, S.E., 2014. A study on the variation of c-Si solar cell parameters under 8 MeV electron irradiation. Solar Energy Materials and Solar Cells 120, 191–196. <https://doi.org/10.1016/j.solmat.2013.08.043>

C6) In the section 3 “Results and discussions” given photo J-V curves of solar cells under AM1.5G condition before and just after and after 52 months of electron irradiation with different doses. It is not clear why just after electron irradiation the FF values do not change with irradiation dose, while the J_{sc} values decrease. When measurements are conducted 52 weeks after irradiation, J_{sc} remains unchanged, while FF decreases.

A6) We appreciate the reviewer’s detailed observation regarding the changes in J_{sc} and FF values before, just after, and 52 weeks after electron irradiation.

The unchanged FF values just after irradiation, despite a decrease in J_{sc} , can be explained by the nature of radiation-induced damage. Electron irradiation primarily introduces defects in the bulk and at interfaces, which influence carrier recombination rates. The initial decrease in J_{sc} is likely due to increased recombination and reduced carrier lifetime. However, the FF value may remain unchanged immediately after irradiation because the changes in series and shunt resistances—key factors that influence FF—are minimal at this stage or are balanced out.

After 52 weeks, the decrease in FF could be attributed to the evolution of defect states over time, which affects the electrical properties of the solar cell. Radiation-induced defects may undergo annealing or recombination (defect-defect recombination) with time, altering the series and shunt resistances and leading to a degradation in FF. On the other hand, the stability of J_{sc} at this stage suggests that the carrier collection mechanisms have stabilized, likely due to a partial recovery of carrier lifetimes or reduced defect activity over time.

We acknowledge that this behavior is complex and depends on multiple factors, including the dose of irradiation, defect dynamics, and the material properties of the solar cell. Further studies focusing on the time-dependent behavior of defects and their impact on electrical parameters would provide deeper insights into this phenomenon.

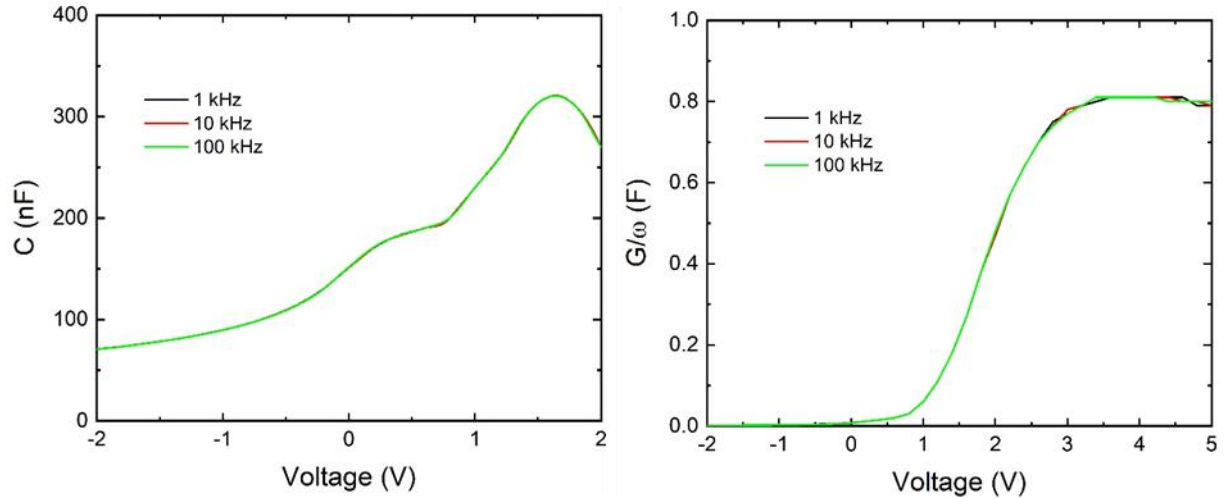
C7) It would be better if could provide data on the lifetime or diffusion lengths of minority carriers before and after electron irradiation, since these parameters are the main ones. On page 12, line 40-47.

A7) By using EQE curves of the cells, we calculated diffusion lengths of the cells for long wavelength limits. The results of calculations are presented in the manuscript.

C8) It would be better if could provide information about the energy, capture cross-section and concentration of defects in the silicon substrate that have formed after electron irradiation

A8) We thank to reviewer for his/her valuable comment. Actually, measurements were taken between 1 kHz to 100 kHz frequency range. However, any change has been observed in the curves of different frequency. Below C-V and G-V measurement results one of the unirradiated cells is given for 1 kHz, 10 kHz and 100 kHz. The lack of significant variation between 1 kHz and 100 kHz suggests that the dominant processes are fast and not limited by carrier trapping or slow defect dynamics. Which may be due to the edges of the cells. When cells cut from a full wafer cell, the edges of the cells degraded, and metal residues or metal/Si phases may form around the edge. Which could screen the response of the defects with respect to frequency change under overall response of the cells. The C-V and G/ ω -V measurements at 100 kHz

provide macroscopic insight into the electronic behavior of the irradiated cells, primarily revealing overall changes in carrier transport and defect-related recombination mechanisms. However, the specific energy levels, capture cross-sections, and concentrations of defects require additional frequency-dependent or temperature-dependent measurements for precise extraction. Also detailed DLTS measurements required for detailed defect analysis.



- We report effects of electron irradiation on c-Si solar cells with varying electron doses.
- Irradiation effects studied through electrical and spectral response measurements in a complementary way.
- The performance of aged c-Si solar cells was investigated again after 52 months later.
- Room temperature self-healing effect was observed after 52-month period of irradiation.
- Remarkable enhancement was observed in the blue response of the cells after 52-month period compared to the unirradiated and just irradiated cell responses.

Observation of Self-Healing and Blue Response Enhancement in c-Si Solar Cells Exposed to Electron Irradiation

Ismail Kabacelik^{1*} Mustafa Kulakci^{2,3}

¹ Department of Medical Services and Techniques, Vocational School of Health Services, Bartın University, 74100, Bartın, Turkey

² Department of Physics, Eskisehir Technical University, 26470 Eskişehir, Turkey

³ Institute of Earth and Space Sciences, Eskisehir Technical University, 26470, Eskişehir, Turkey

Abstract

The effects of electron irradiation on the performance of mono-crystalline silicon (c-Si) solar cells were investigated by examining various electron doses, ranging from 225 to 900 Gy, with an energy of 8 MeV. The study focused on dose-dependent degradation in cell behavior resulting from irradiation. Detailed analysis was conducted through dark and illuminated current-voltage (I-V) measurements, external quantum efficiency (EQE) measurements, capacitance-voltage (C-V) measurements, and conductance-voltage (G/ω -V) measurements. The observed degradations were thoroughly analyzed, quantified, and discussed by comparing the results obtained from complementary electrical and optical characterizations of the cells before and after irradiation. The experimental findings indicated that the degradation in cell parameters was attributed to irradiation-induced defect formations in the base layer. However, the devices were found to be resilient to defect formations in the emitter and near the depletion edge of the base. After 52 months of irradiation, significant self-healing effects and improvements in blue response were observed in the cells, likely due to additional positive charge formation in the nitride layer from oxynitride formation in the ambient atmosphere over time, accelerated by radiation damage. This was confirmed by both illuminated I-V and EQE measurements.

Keywords: Solar cell; Electron irradiation; Aged c-Si solar cell; Electrical characterization; Self-healing effect

* Corresponding author: Ismail Kabacelik
E-mail address: ikabacelik@gmail.com

1. Introduction

Photovoltaic (PV) has been a fast-growing market for the last decades to close the gap in increasing electrical energy demand in a sustainable way by using solar energy as being the largest among renewable energy sources. Today, the PV industry is overwhelmingly dominated by c-Si technology with a market share of over 90% in terrestrial applications (Yu et al., 2022). Although c-Si cell technology was the pioneer of the space utilization of PV and has kept its dominance in this area for a long time, its dominance has been superseded by group III-V semiconductor cell technology. Recently, Si has regained significant interest due to the widespread progress in space and aerospace technologies, which require large-scale and relatively cost-effective installations. Highly efficient new cell technologies based on hybrid integration of Si and III-V technologies either by mechanical or wafer bonding techniques have been pursued to provide a viable solution for flourishing market requirements in a reliable and cost-effective way (Cariou et al., 2018; Medjoubi et al., 2021; Mizuno et al., 2022). Besides its cost-effectiveness, Si is a good alternative to Ge as a bottom cell due to its superior properties much suitable for space environment, such as mechanical robustness, radiation and temperature tolerances (Essig et al., 2017; Medjoubi et al., 2021; Sharma et al., 2022; Yu et al., 2022).

Solar cells used in space applications are exposed to high-temperature cycles, wide range of charged and uncharged radiations that adversely affect cell performances (Hamache et al., 2016; Kabacelik et al., 2017; Luft, 1964; Nikolić et al., 2015; Pellegrino et al., 2019; Sato et al., 2009; Yang et al., 2011). Therefore, cells to be used in that harsh environment inevitably require not only high-efficiency values with a high watt/kg ratio but also high tolerances to that hard condition for stable and long-term reliable use in space platforms. Today only a few material systems can provide all these requirements and prove themselves over long-term use in numerous different tasks. While c-Si cells show moderate sensitivity to radiation-induced degradation compared to thin-film and multi-junction cells, their widespread adoption, mature technology, and relatively low cost make them a practical choice in various radiation environments. When comparing c-Si solar cells with other types such as III-V group solar cells, Cu_x(In_{1-x}Ga_x)Se₂, CdTe/CdS, and perovskite solar cells for space applications, several key factors come into play, particularly in terms of efficiency, radiation hardness, cost-effectiveness, functionality over flexibility and lightweightness (Jasenek and Rau, 2001; Kawakita et al., 2002; Krishnan et al., 2009; Lang et al., 2016; Yang et al., 2020). c-Si solar cells, although widely used in terrestrial environments due to their cost-effectiveness and established manufacturing processes, exhibit moderate radiation resistance (Hamache et al., 2016; Mizuno et al., 2022). Their performance can degrade over time when exposed to high-energy space

radiation, leading to an increase in defect density and a reduction in carrier lifetime. In contrast, III-V group solar cells, known for their high efficiency, particularly in multi-junction configurations, are far superior in terms of radiation resistance (Li et al., 2021; Raya-Armenta et al., 2021). These cells are specifically designed to withstand the harsh radiation environment of space, maintaining their performance over extended periods. Cu(In,Ga)Se₂ solar cells, while flexible and efficient, offer higher radiation resistance than III-V cells (Jasenek and Rau, 2001; Kawakita et al., 2002). Consequently, their performance may deteriorate faster when subjected to the intense radiation in space. Similarly, CdTe/CdS solar cells, with a relatively simple manufacturing process and good efficiency, also show limited radiation tolerance (Verduci et al., 2022). This makes them less ideal for long-term missions in various radiation environments, where maintaining performance is critical. Perovskite solar cells, which have gained attention due to their high efficiency and lightweight properties, face challenges in terms of radiation resistance (Lang et al., 2016; Li et al., 2022; Yang et al., 2020). Their performance tends to degrade under prolonged exposure to space radiation, and their long-term stability is still under investigation.

As the irradiation by high energy particles introduces defect formations in solar cells (Srour et al., 2003; Zhang et al., 2020), it is critical to understand the behavior of the cells that are exposed to those radiations for the reliability and longevity of the utilization. Mainly two effects occur in the cell structure as a result of interaction with the energetic particles; the first one is ionization and the second one is displacement damage (Danilchenko et al., 2008; Summers et al., 1995; Zhang et al., 2014). The ionization effect is the generation of electron-hole pairs in the base layer of the cell. The displacement damage is the movement of atoms from their initial position in the crystal lattice to another position where they are electrically inactive. These induced defects produce generally deep energy levels in the band gap of the cell material (Ali et al., 2016; Nikolić et al., 2013). Then those defects mostly act as traps and recombination centers that cause to degradation in lifetime and diffusion length of minority carriers in the base of the cell and could cause to increased resistivity due to a reduction in the majority carriers (Bhat et al., 2014; Oeba et al., 2021; Yan et al., 2020; Zdravković et al., 2011). As a result of all effects, significant degradations could be observed in the output parameters of the cells (Hisamatsu et al., 1998; Shen et al., 2019; Tobnaghi et al., 2014; Weiss et al., 2020).

After successful demonstration on Vanguard I, Si cell had become the indispensable choice of cell technology for space applications for a long time (Essig et al., 2016; Green, 2016; Schnabel et al., 2020). To understand the effects of space conditions on Si cell performance, irradiation studies have been initiated as early as the 60s and keeping its importance up to date

(Junga and Enslow, 1959; Luft, 1964). Those studies that mimicking the space environment have led to the development of more tolerant Si cells in terms of design and material (Schygulla et al., 2022; Verduci et al., 2022). Although degradation mechanisms in Si cells are well understood with respect to different aspects of energetic particles like particle type, fluence, energy etc., there is a huge room about recovery after irradiation, especially on self-healing effects without applications of any external agents on the cells.

High-energy electron-induced degradation of Si solar cells has been extensively studied and reported in the literature (Ali et al., 2016; Babaee and Ghozati, 2017; Hamache et al., 2016; Kabaçelik, 2023; Liao et al., 2023; Sahin and Kabacelik, 2018; Yamaguchi et al., 1999). Yamaguchi et al. have observed a gradual decrease in I_{sc} under 1 MeV electron irradiation at fluences up to $5 \times 10^{16} \text{ e/cm}^2$, followed by a sharp decline to zero at a fluence of $1 \times 10^{17} \text{ e/cm}^2$ (Yamaguchi et al., 1996). Krishnan et al. reported a notable alteration in the diffusion component of the saturation current in Si photodetectors exposed to 8 MeV electron radiation at doses up to 100 kGy (Krishnan et al., 2007). It has been reported that fluences of 1 MeV electrons greater than 10^{16} cm^{-2} induce an anomalous increase in I_{sc} of Si solar cells, followed by a sudden decrease and cell failure, due to a decrease in carrier concentration in the base region and a reduction in the minority carrier diffusion length (Imaizumi et al., 1999). Bhat et al. have related the increase in the interface density of states in Si solar cells exposed to 8 MeV electron radiation to a decrease in carrier concentration, attributing this to the trapping of charge carriers caused by an increase in radiation-induced trap centers, as determined through C-V and G/w-V analyses (Sathyaranayana Bhat et al., 2015).

High-energy particle irradiation induces defects such as vacancies, interstitials, and complex structures involving oxygen (O), carbon (C), and boron (B) impurities (Feklisova et al., 2013; Liao et al., 2023; Matsuura et al., 2006). Prominent defect complexes include vacancy-carbon-oxygen (V-C-O), interstitial-carbon–interstitial-oxygen (Ci–O_i), boron-interstitial–oxygen (Bi–O_i), and vacancy-oxygen-boron (V-O-B) complexes (Liao et al., 2023; Matsuura et al., 2006; Yamaguchi et al., 1999). Additionally, vacancy-related centers like the A-center (V–O) and divacancy states (V–V) are significant contributors to recombination losses (Radu et al., 2013; Yamaguchi, 2001; Zh Karazhanov, 2000). These defects adversely affect carrier lifetimes and increase recombination rates, underscoring the importance of understanding their formation and behavior to enhance solar cell resilience in high-energy environments, such as space.

In this study, the effects of 8 MeV electron irradiation on the c-Si solar cell performance have been investigated extensively and in detail for different doses. Electrical and optoelectronic characterization techniques have been used to evaluate the electron-induced degradations in the device characteristics of the cells before and after irradiation. After 52 months of irradiation cell parameters were measured again at the same conditions as before to reveal any possible effect of time. A remarkable self-healing effect has been observed in the cells kept at room temperature whose strength depends on electron dose and quantified through recovery in the cell parameters. The quantification of recovery in the cell parameters has been reached via comparative assessment of the successive measurement results of unirradiated and irradiated cells. Moreover, significant enhancement was observed in the blue response of the cells after 52 months of irradiation compared to that of unirradiated ones, which could shed a light to understand and develop new insights for the passivation of Si solar cells.

2. Materials and methods

The solar cells were fabricated using Czochralski-grown (Cz) mono-crystalline, (100) oriented, p-type Si wafer (boron-doped $\sim 5 \times 10^{16} \text{ cm}^{-3}$) with a resistivity of 1-3 $\Omega \cdot \text{cm}$, with a thickness of 160 μm , and with dimensions of 156 mm x 156 mm. The emitter layer (n) was formed by phosphorus diffusion with a concentration of $5 \times 10^{20} \text{ cm}^{-3}$. Details of the cell fabrication process are given elsewhere Ref (Es et al., 2016) and (Kulakci et al., 2013). A schematic diagram illustrating the overall structure of the fabricated solar cell used in this study is shown in Fig. 1.

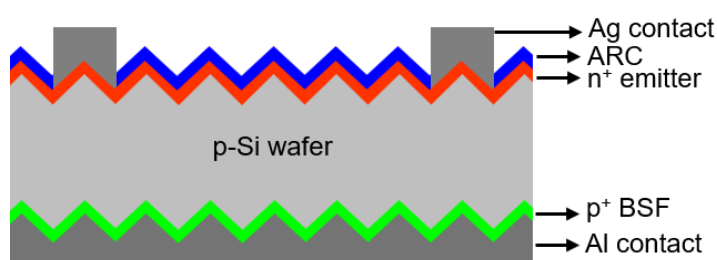


Figure 1. Schematic structure diagram of the fabricated Si solar cells.

Following the device fabrication, the cell was cut into smaller pieces with an area of 2.8 cm^2 by using a laser. Then, the electrical characteristics and spectral responses of each cell were measured before and after electron irradiation. The measurement done on irradiated cells after 1 day of irradiation and refers to just after irradiation in the text. Dark I-V measurements were performed by Keithley 2440 source-meter. Illuminated I-V measurements were performed

under AM1.5G condition using Abet 2000 solar simulator. The spectral response of the cells was measured in a wavelength range of 300 - 1100 nm and with an interval of 10 nm using Newport QuantX-300 quantum efficiency measurement system. C-V and G/ ω -V measurements were performed under dark conditions using an HP 4192A LF impedance analyzer, with an AC signal of 100 kHz frequency and 50 mV amplitude. All measurements were carried out at room temperature under atmospheric conditions (the pressure around 0.92 atm, humidity about 45%-50%).

Solar cells were exposed to electrons with an energy of 8 MeV using a modified clinical linear accelerator (cLINAC, Philips SLI-25 LINAC). In the cLINAC system, a 50 keV potential difference was applied to the electron gun to enable electron emission. The steering and focusing of the electrons, accelerated at approximately 3 GHz by radio frequency, are accomplished using standard magnetic and electrostatic components. The 8 MeV electron energy from the LINAC was directed at the solar cells with a uniform beam profile, which were positioned to face the beam directly to ensure that all samples received an equal irradiation dose. The dose rate was maintained constant at 7.5 Gy/min, provided the distance between the solar cell sample and the radiation source remained unchanged. Detailed information on cLINAC can be found at Ref (Boztosun et al., 2015). Four solar cells were chosen and separately irradiated with different doses of 225, 450, 675 and 900 Gy which are corresponding to 1.8×10^{14} to 7.2×10^{14} cm⁻² for the lowest and highest fluence of electron respectively. All irradiation processes were carried out under ambient conditions at room temperature.

In this study, electrical and optical properties of c-Si solar cells were systematically studied by means of dark and illuminated I-V, EQE, C-V and G/ ω -V measurements before and after 8 MeV electron irradiation at various applied doses. After irradiation solar cells were kept at ambient conditions at room temperature for 52 months and were characterized again to see possible recovery/degradation in time.

3. Results and discussions

Room temperature dark I-V measurement results of solar cells before, just after irradiation and after 52 months of irradiation for different electron doses are shown comparatively in Fig. 2. Diode ideality factors calculated by using single diode model from these curves are given in Table 1. As observed in the table, with the radiation dose increases, the diode ideality factor also increases, suggesting the formation of generation-recombination (G-R) levels by the irradiation-induced defects within the bandgap of Si, which impacts the diode's electrical behavior (Oeba et al., 2024). After 52 months of irradiation, ideality factors

close towards the unirradiated values which indicates the annihilation of some of those levels in 52 months period of keeping the cells at room temperature. The effect of electron irradiation is also clearly seen in the reverse bias regime (Fig. 2), generation current increases in accordance with the dose level which is also consistent with the increase in ideality factor towards 2 (and over) in the forward bias regime because of increased recombination current with the act of these defects (Bodunrin and Moloi, 2024). As in the case of forward bias, the self-annihilation effect has been also seen in reverse bias after 52 months, excess generation currents reduced to the level of unirradiated devices.

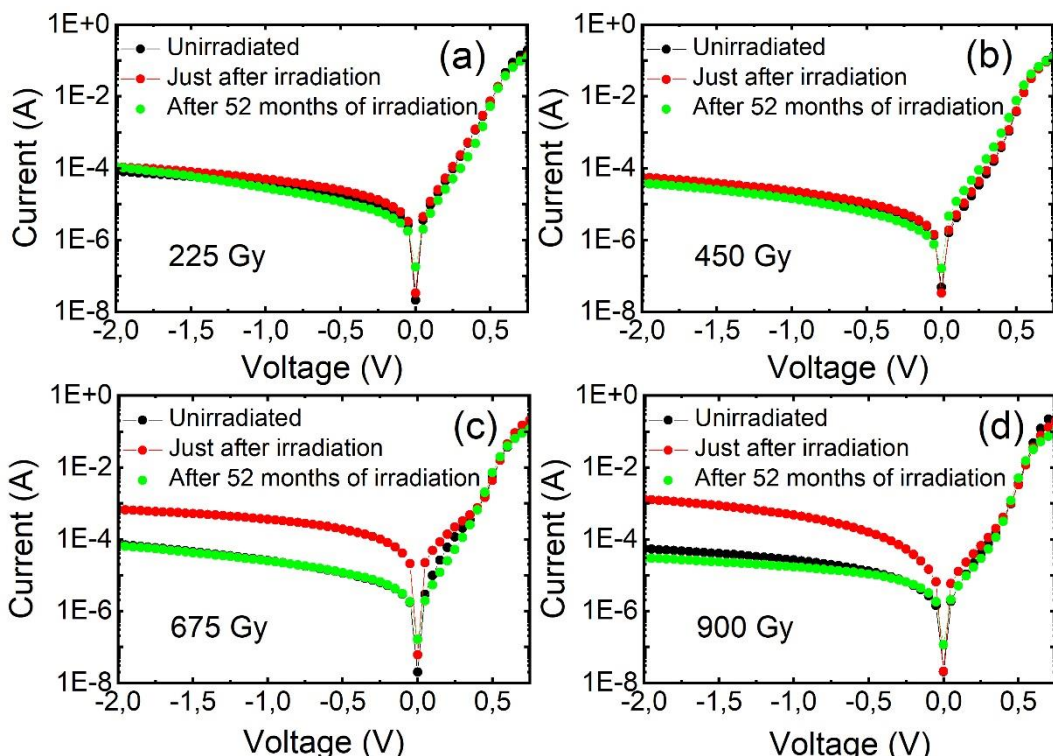


Figure 2. Dark I-V curves of the cells measured at room temperature for different doses of electron irradiation.

Table 1. Calculated diode ideality factors of the cells.

	225 Gy	450 Gy	675 Gy	900 Gy
Unirradiated	1.71	1.67	1.62	1.76
Just after irradiation	1.86	1.94	2.18	2.43
After 52 months of irradiation	1.74	2.08	1.95	2.13

The illuminated I-V characteristics of solar cells under AM1.5G condition before and after irradiation with different electron doses are shown in Fig. 3. Calculated cell parameters using data of this figure are presented in Table 2. The mismatch in the results of different cells could be attributed to the effect of laser cut. The parameters of the full wafer cell before laser cut were 17.6 %, 612 mV, 36.1 mA/cm² and 79.7 % for η , V_{OC} , J_{SC} and FF, respectively. The laser cut induced edge degradation is clearly seen when comparing the cell parameters of full wafer cell and small cells used in this study. As clearly seen from figure and table, there is a reduction in both J_{SC} and V_{OC} values of cells after irradiation where the level of reductions follows an increase in electron dose. The decrease in J_{SC} and V_{OC} is due to the electron-induced defects that act as recombination centers for the light-generated carriers before diffusing to the depletion region. As the density of defects increases with the radiation dose, carrier loss becomes more pronounced in a monotonous way (Bodunrin and Moloi, 2022; Giesecke et al., 2011; Horiuchi et al., 2000), even for aggressively higher dose levels anomalous degradation in cell outputs could be observed (Morita et al., 1997). When considering the energy of the impacting electrons, the origin of those defects assumed to be displaced Si atoms from their lattice sites (Bhat et al., 2015), and manifest themselves on the carrier's lifetime/diffusion length, especially in the base layer of the cells (Ashry and Fares, 2003; Bhat et al., 2014; Kuendig et al., 2003; Taylor et al., 1997). After irradiation, cells were kept at ambient conditions at room temperature for 52 months to see any recovery/degradation in time. When looking at the comparative I-V curves in the figure, one can easily see varying self-recovery behavior in the cell parameters depending on radiation dose, which is more remarkable in the J_{SC} . The degree of improvement is the greatest in the cell irradiated with the lowest dose of electron and is monotonously decreasing with the increase in dose level. Observed room temperature self-healing effects in the J_{SC} discussed in detail below together with EQE results. A small improvement was also observed in V_{OC} values, but it is not substantial as in the case of J_{SC} .

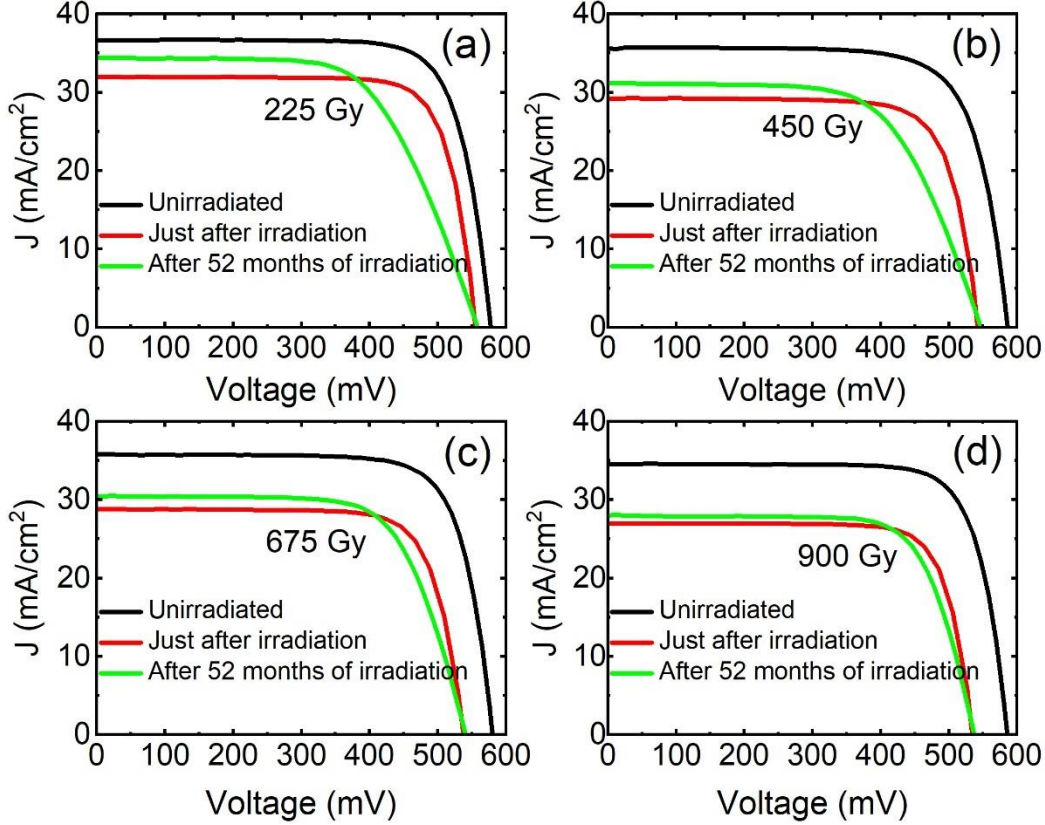


Figure 3. Illuminated (AM1.5G) I-V curves of the cells for different doses of electron irradiation.

Table 2. Basic cell parameters obtained from illuminated I-V given in Fig.3

Dose (Gy)	Unirradiated				Just after irradiation				After 52 months of irradiation			
	Voc (mV)	Jsc (mA/ cm ²)	FF (%)	η (%)	Voc (mV)	Jsc (mA/ cm ²)	FF (%)	η (%)	Voc (mV)	Jsc (mA/ cm ²)	FF (%)	η (%)
225	578	36.7	77.1	16.3	553	31.9	78.7	13.9	558	34.4	62.9	12.1
450	586	35.6	74.9	15.6	542	29.3	76.5	12.1	546	31.2	63.7	10.8
675	580	35.8	76.5	15.9	538	28.8	76.7	11.9	540	30.4	69.5	11.4
900	585	34.6	77.8	15.7	534	26.9	78.4	11.3	537	27.9	73.4	10.9

The evolution of the tabulated cell parameters is visualized in Fig. 4 to easily follow the effects of electron dose on the performance of the cells. Fig. 4(a) shows the normalized parameters of just-irradiated cells; the normalization done on each irradiated cell parameters by their unirradiated values separately as each cell has nonequivalent device characteristics. The 0 Gy represents the normalization of unirradiated cell parameters by themselves separately for each cell as well. Therefore, Fig. 4 (a) represents the relative change of the cell parameters

under varying irradiation dose with respect to their respective initial values. As seen in the figure, there is an obvious performance loss which increases with increasing dose level. The loss in conversion efficiency is 15% for the lowest dose level of 225 Gy and reaches 28% for the highest dose level of 900 Gy with respect to their initial values. The rate of efficiency loss goes to decrease with an increase in each successive dose level. It is observed that J_{sc} of the devices is more delicate to the electron irradiation compared to V_{oc} values. The loss in J_{sc} is 13% and 22% for the lowest and highest electron doses, whereas those loss are only 4% and 8% for V_{oc} for these subscribed dose levels respectively. Irrespective of the level of dose, the loss in efficiency is mainly determined by the degradation in J_{sc} rather than degradation in V_{oc} . Which could imply that irradiation is most effective in bulk region of the devices rather than surface or close surface regions. The degradation in cell parameters, especially in J_{sc} will be elaborated deeply with the conjunction of EQE measurement results. Any degradation has been observed in the FF values after irradiation, indeed slight enhancements are clearly seen. Similar behavior for FF-dose dependence was observed in Si solar cells irradiated with 8 MeV electron using much higher electron dose than that used here (Bhat et al., 2014).

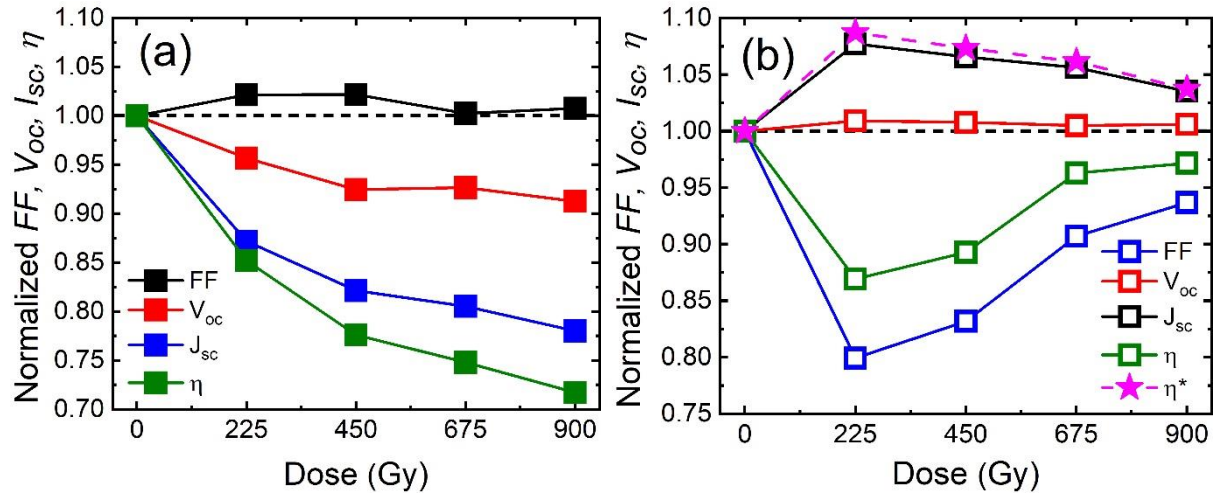


Figure 4. Evolution of normalized cell parameters: **(a)** values of just irradiated case, normalized by their unirradiated values, **(b)** values of after 52 months of irradiation, normalized by just irradiated values. The dashed lined curve in **(b)** represents the projected normalized efficiency (η^*) of the cells after 52 months, under the assumption FF values of just irradiated cells were preserved without any degradation.

Fig. 4(b) shows the normalized parameters of the cells measured after 52 months of irradiation. Normalizations were done on each parameter of the cells obtained after 52 months of irradiation with respect to their just irradiated values. In this case normalization is done to

see the relative changes in the cell parameters after 52 months of irradiation compare to their just irradiated values. The 0 Gy represents the normalization of just irradiated cell parameters with themselves separately for each cell as well. When looking at the change in V_{OC} and J_{SC} values, the enhancement is seen compared to the just irradiated values. Which indicates room temperature self-healing effect in the cells without applying any external agent like heat treatment etc., the cells were only preserved in ambient conditions for 52 months. As clearly seen, there is a remarkable recovery in J_{SC} values which could imply that some of the defects generated in the bulk due to irradiation, especially those that are not very stable had been cured over the 52 months period (Bhat et al., 2014; Radu et al., 2013). The observed recovery is more pronounced in J_{SC} values compared to the recovery seen in the V_{OC} values. The relatively small amount of enhancement seen in the V_{OC} values is almost independent of the irradiation dose. On the other hand, the relative enhancement in J_{SC} is inversely proportional to the dose level. The maximum level of enhancement in current is seen in the cell that was irradiated with the lowest amount of electron dose, then the percentage of recovery decreases monotonously with an increase in electron dose. The calculated percentage recovered part of J_{SC} values due to self-healing is given in Table 3. The recovery in J_{SC} is 16.2% for the highest irradiation dose, it monotonously increases with decrease in dose level and reaches as high as 52.6% for the lowest dose. More details on the recovery in current will be given in the EQE part. Although one expects enhancement in the conversion efficiencies (compared to just irradiated values) regarding the recovery in corresponding V_{OC} and J_{SC} values, the calculated efficiency values do not reflect the expectations as seen in Fig. 4(b). The reduction in efficiencies after 52 months solely depends on the degradation in FFs. As clearly seen in the figure, the efficiency-dose curve directly follows the behavior of FF-dose curve with almost the same functional dependence. The main reason for FF degradation after 52 months of irradiation was found to be an increase in the series resistance of the cells (Fig. 5). The shunt resistances had insignificant changes after 52 months compared to ones obtained from the measurements just done after irradiation of the cells (not shown here), this may be due to screening effect of the degraded cell edges by laser cut. For the case just after irradiation, series resistance slightly increases with an increase in dose level. Contrary to just-irradiated cells behavior, the series resistance decreases in a monotonous way with an increase in irradiation dose (See Fig. 5). Assuming that, the FF of the irradiated cells were preserved without any degradation during this 52-month period, the projected conversion efficiencies were calculated and are shown as a dashed curve in Fig. 4(b). Based on this projection, efficiency losses caused by irradiation partially recovered, with 8.7% recovery for the lowest dose and 3.7% for the highest dose. Notably, the

improvement in efficiency is primarily attributed to the recovery of the short-circuit current, as evidenced by the comparison between the current-dose and efficiency-dose curves in Fig. 4(b) across different irradiation levels.

Table 3. Calculated loss and recovery in J_{SC} values from illuminated I-V measurements (Fig. 3) for different radiation doses. J_{SC0} , J_{SC1} and J_{SC2} are the short circuit current densities of the cells before irradiation, just after irradiation and after a 52-month period of irradiation respectively.

Dose (Gy)	Loss in J_{SC} ($J_{SC0} - J_{SC1}$) (mA/cm ²)	Recovery in J_{SC} ($J_{SC2} - J_{SC1}$) (mA/cm ²)	Percentage in J_{SC} recovery (%)
225	4.70	2.47	52.6
450	6.37	1.92	30.1
675	6.97	1.62	23.2
900	7.60	1.23	16.2

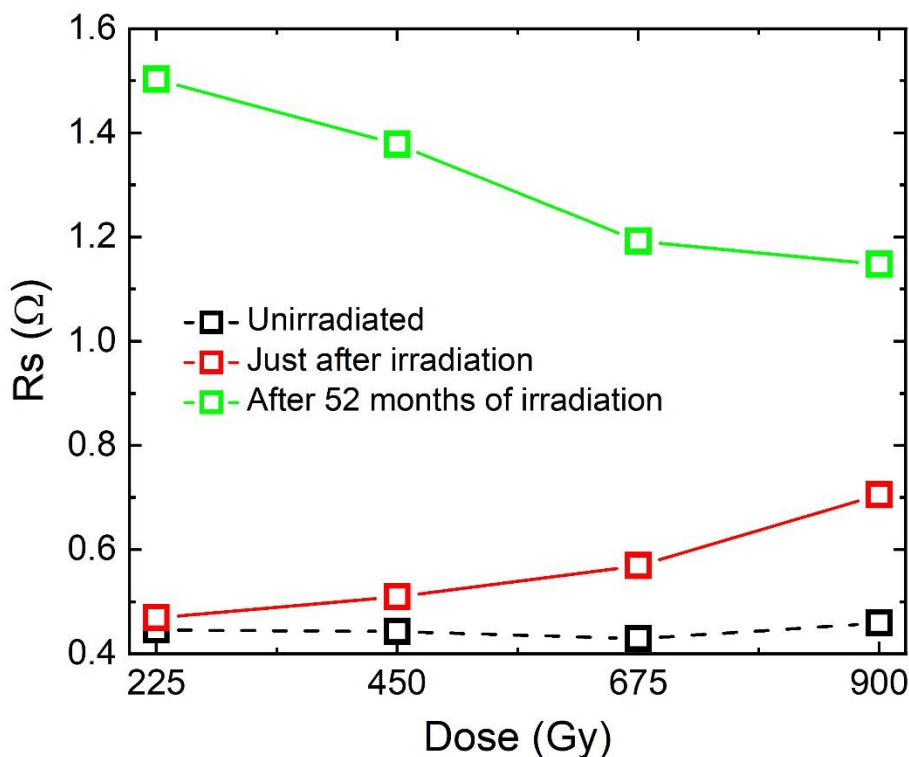


Figure 5. Irradiation effects on series resistance of the cells with varying electron doses from illuminated I-V measurements.

EQE measurement is a valuable method to understand the behavior of the cell with respect to specific region of incoming photon wavelength. To thoroughly investigate the

degradation effects of electron irradiation on the cells and to determine the potential mechanisms responsible for the self-healing effects observed in the recovery of short circuit current, EQE measurements were conducted. The findings of these measurements are presented comparatively in Fig. 6.

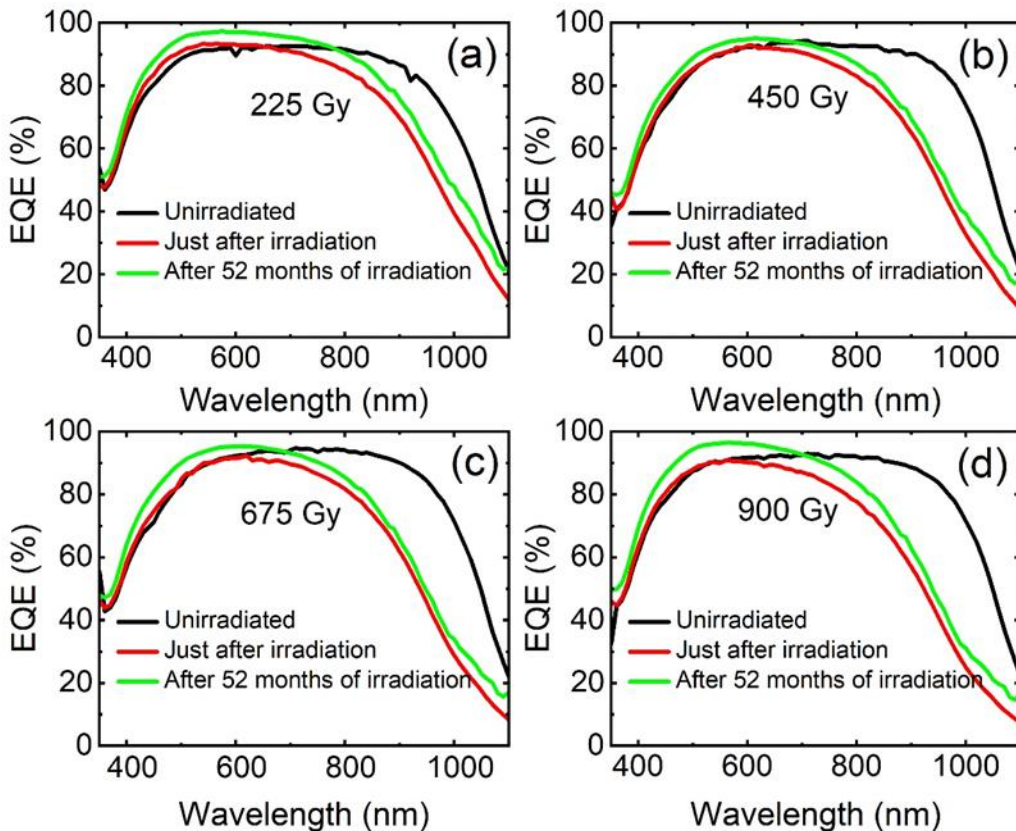


Figure 6. The EQE spectrum of the cells for different irradiation levels.

Based on the results shown in Fig. 6, a significant decrease in EQE values can be observed in the long-wavelength region of the spectrum, and this loss in the red response becomes more prominent with increasing levels of irradiation. It is noteworthy that electron irradiation did not cause any changes in the reflectivity properties of the cells. To see any effect of storage for 52 months on the cell behavior, EQE of unirradiated another cell is given in Fig. 7(inset). Any observable changes (degradations or enhancements) were detected in the EQE results of an unirradiated cell measured at the beginning of the study and after 52 months. Therefore, the reductions in EQE (Fig.6) are directly attributed to the decline in carrier collection due to defects generated by irradiation in the active regions of the devices. On the other hand, EQE results suggest that solar cells have high tolerance to defects in the blue response region of the spectrum as the light absorbed close to the surface.

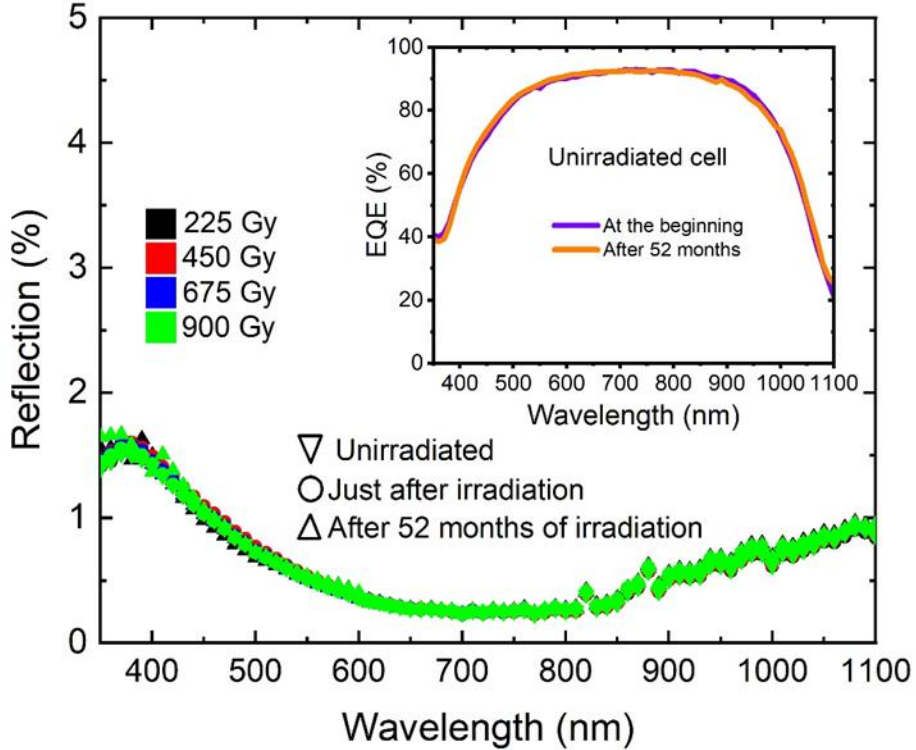


Figure 7. Comparative reflection spectrum of the cells. The inset shows the EQE spectrum of an unirradiated sample at the beginning and after 52 months.

Upon examination of Fig. 6, a distinct demarcation can be observed on the high-energy side of the curves. Beyond this point, towards the lower wavelength region of the spectrum, no detrimental effects on the cell response were observed. In fact, a very slight improvement can be seen in the curves. For the lowest dose (225 Gy), the border of onset is approximately at a wavelength of 654 nm, while for higher doses, this onset systematically shifts towards lower wavelengths and reaches around 535 nm for the highest irradiation dose (900 Gy). Considering the absorption depth of these wavelengths of light in Si, the onset points, at which the loss of minority carrier collection begins, are situated at approximately 3.5 μm from the surface of the cells for the lowest dose, and this depth decreases to around 1.1 μm for the highest dose. The cells have an emitter depth of 500 nm, and the depletion layer width in the absorber region is calculated to be around 300 nm. This indicates that for the highest irradiation dose, recombination loss begins in the immediate vicinity of the depletion region, and as the dose decreases, the loss moves deeper into the absorber. Based on the behavior of the curves, it can be inferred that there is no carrier loss observed in the emitter and depletion layers, even when subjected to the highest dose of electron irradiation, as compared to the response of unirradiated cells. The EQE results suggest that the degradation observed in the solar cells after electron irradiation can be attributed to the formation of defects in the base layer (Bhat et al., 2014;

Yamaguchi, 2001). These defects cause a reduction in the minority carrier diffusion length or minority carrier lifetime, resulting in carrier collection loss due to recombination (Babae and Ghozati, 2017). In the EQE results, the decrease in efficiency for longer wavelength photons in the spectrum is mainly attributed to absorption deeper in the absorber layer and towards the back contact, which results in significant loss of carrier collection, and this loss behavior is found to depend on the irradiation dose (Khan et al., 2003; Krishnan et al., 2007; Matsuura et al., 2006). The observed carrier loss behavior in EQE is well-correlated with the dose dependence of J_{sc} values obtained from the illuminated I-V curve of the cells just after irradiation (see Fig. 3, Fig. 4, and Table 3).

Fig. 6 also shows the EQE measurement results of the cells after 52 months of irradiation. There is an enhancement in the EQE response for all dose values across the entire spectrum compared to the results obtained immediately after irradiation. A significant increase in the blue response of the cells is observed in the curves, which is even higher than the blue response of the unirradiated cells. This enhancement in blue response could be due to the formation of positive charges in the silicon nitride layer over time, which might cause field effect passivation on the emitter surface by pushing minority carriers (holes) away from the interface. It is well known that excess positive charges related with K (+) center in silicon nitride serve as an effective field-effect passivation in silicon solar cells especially on n-type emitter (Leguijt et al., 1996; Lelièvre et al., 2009; Sharma et al., 2013). At room temperature, ambient oxidation could form oxynitride formation in silicon nitride film which enhances extra positive charge formation over oxygen-correlated bond defects in time which may boost field effect passivation over 52 months period (Raider et al., n.d.; Schmidt and Aberle, 1999). Most probably due to radiation-induced damages this charge formation could be boosted and result in good surface passivation which is not observed in unirradiated cell (Robertson, 1993). Upon examining Fig. 6, it can be observed that the onset of carrier loss shifts to higher wavelengths compared to the results immediately after irradiation, with the switch occurring from around 654 nm to 786 nm for the lowest dose and from about 535 nm to 700 nm for the highest dose. In terms of the absorption depth of these wavelengths, the onset of carrier loss shifts from 3.5 μm to 9.6 μm for the lowest dose and from 1.1 μm to 5.0 μm for the highest dose, respectively. For doses in between, the recovery in EQE response is slightly lower compared to these extremes. The EQE curves suggest that the improvements in carrier collection could be attributed to the reordering of radiation-induced defects over time at room temperature, which could be referred to as the room temperature annealing or self-healing effect. The enhancement

and partial recovery in EQE over 52 months (Fig. 6) are consistent with the recovery in short-circuit current behavior (Fig. 3 and Fig. 4) obtained from illuminated I-V measurements.

As the EQE is the spectral distribution of photocurrent, short circuit current values of the cells also calculated using Eq. 1.

$$J_{sc} = \int EQE(\lambda) J_{\gamma,AM1.5G}(\lambda) d\lambda \quad (1)$$

where, $J_{\gamma, AM1.5G}(\lambda)$ is the incident photon current density per wavelength interval, derived from AM1.5G data taken from ASTM G173-03 reference spectrum.

To determine the loss and the self-healing effects in currents, the J_{SC} values calculated from EQE curves of cells for the cases of unirradiated, just irradiated, and after 52 months of irradiation are compared in Table 4, in a similar way as done in the illuminated I-V measurements. As seen from the table, the irradiation loss in current increases monotonously with an increase in dose level which is consistent with results that were obtained from the solar simulator measurements (Table 3). However, the degree of current losses measured under a solar simulator is slightly higher than ones calculated from EQE measurements. Based on the calculations using EQE spectrum, in a 52-month period after irradiation, 81.5% of the loss in current recovered back for the device subject to the lowest electron dose and it is about 44.3% for the highest dose respectively. For the dose levels in between them, the calculated recovery in current is relatively low compared to these extremes. The recovery in short circuit currents calculated from EQE measurements is higher than that obtained from solar simulator measurements (Table 4 and Table 3). The differences observed loss in current levels just after irradiation and recovery in currents due to self-curing effects between the solar simulator and EQE measurement might be results of difference in illumination area on the cells. In solar simulator measurements the whole area of the cells was illuminated, on the other hand in EQE measurements the illumination area was only 2 mm². The cells used here are laser cut from a 243 cm² cell into a small size of 2.8 cm². The laser cut processing unavoidably damages the edges of the cells, which could introduce extra recombination and leak pathways, and this could lower the current in solar simulator measurement due to extra carrier losses over the defective edges.

1 **Table 4.** Calculated loss and recovery in J_{SC} values from EQE measurements (Fig. 6) for
 2 different radiation doses. J_{SC0} , J_{SC1} and J_{SC2} are the short circuit current densities of the cells
 3 for unirradiated, just irradiated and after 52 months of irradiation cases respectively.

Dose (Gy)	Loss in J_{SC} ($J_{SC0} - J_{SC1}$) (mA/cm ²)	Recovery in J_{SC} ($J_{SC2} - J_{SC1}$) (mA/cm ²)	Percentage in J_{SC} recovery (%)
225	2.75	2.24	81.5
450	4.62	1.73	37.4
675	5.36	1.89	35.3
900	5.87	2.60	44.3

16 As discussed earlier, there is a partial recovery in the carrier collection efficiency for the
 17 long-wavelength region compared to the significant enhancement observed in the short-
 18 wavelength region. For long wavelengths, where carriers are generated deeper within the bulk
 19 of the material, the collection efficiency is primarily governed by the minority carrier diffusion
 20 length (L). Using the EQE curve, the diffusion length for medium and long wavelengths can be
 21 calculated using Eq. (2) (Basu et al., 1994; Onoda et al., 2002; Saad, 2002).

$$27 \quad 28 \quad 29 \quad \eta = (1 - R) \left(1 - \frac{e^{-\alpha W}}{1 + \alpha L_n} \right) \quad (2)$$

30 Here R is the reflection coefficient, α is the absorption coefficient, W is the depletion width
 31 and L_n is the minority carrier (electron) diffusion length.

34 The calculated minority carrier diffusion lengths for the cells are presented in Fig. 8 for
 35 wavelengths of 800 nm and 900 nm. The data clearly reveal variations in the diffusion length
 36 among samples, which is attributed to the inhomogeneities introduced by the laser cutting
 37 process used to divide the full wafer into individual cells. These inhomogeneities likely result
 38 in differences in the bulk and surface recombination characteristics across the samples.

43 To account for such variations, the results of each sample were analyzed individually,
 44 as was done for the I-V and EQE measurements. By evaluating each cell independently, we
 45 eliminate the confounding effects of sample-to-sample inconsistencies and focus on the relative
 46 changes in diffusion length under different conditions. Table 5 summarizes the relative
 47 percentage changes in diffusion length for each sample, offering a more reliable basis for
 48 comparison. It is observed that the diffusion length consistently increases as the wavelength
 49 changes from 800 nm to 900 nm. This result aligns with theoretical expectations since longer
 50 wavelengths penetrate deeper into the bulk of the Si, where the generation rate of carriers
 51 decreases, making the measurement more sensitive to the bulk diffusion length (Honsberg and
 52 Bowden, 2019).

Comparing the unirradiated state, the immediate post-irradiation state, and the 52-month post-irradiation state, it is evident that irradiation induces a significant reduction in diffusion length, consistent with the introduction of radiation-induced defects that act as recombination centers. However, over time, a partial recovery in diffusion length is observed for both 800 nm and 900 nm wavelengths. This room temperature recovery could be attributed to the annealing of some radiation-induced defects or a reduction in their recombination activity under ambient storage conditions.

The degree of recovery is more pronounced for the long-wavelength measurements (900 nm), suggesting that bulk recombination processes are more affected by defect annealing than surface recombination. These results highlight the critical role of diffusion length as a parameter for assessing the impact of irradiation and subsequent recovery in Si solar cells. The observed trends in diffusion length across different wavelengths and irradiation conditions provide valuable insights into the material's bulk properties and the long-term effects of radiation-induced defects. These findings underscore the importance of independently analyzing each sample and considering relative changes to draw reliable conclusions, particularly when dealing with inhomogeneous samples such as those cut from a full wafer.

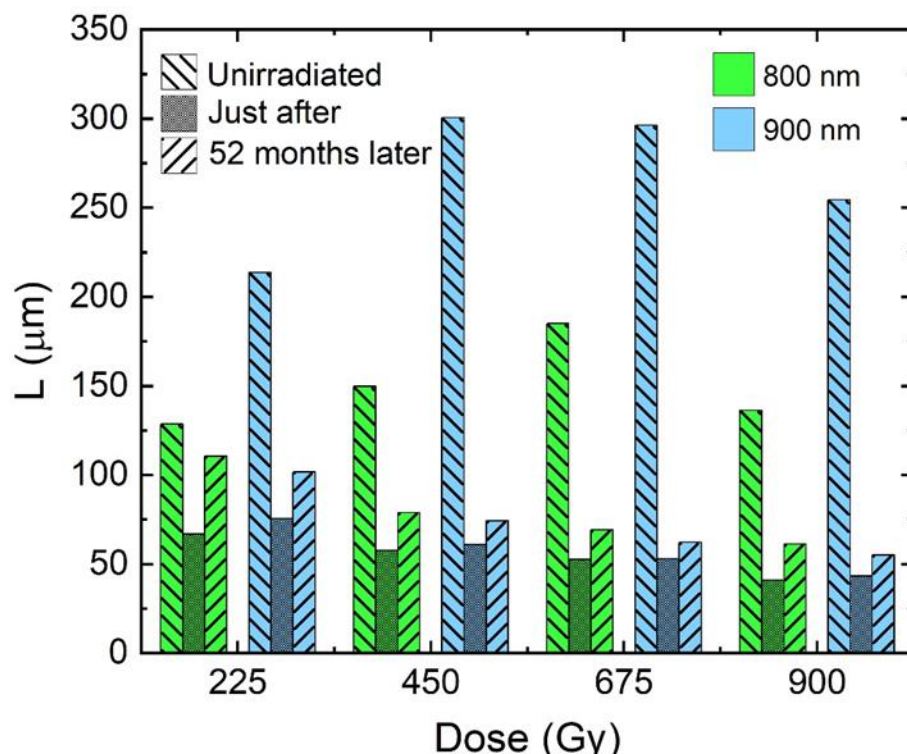


Figure 8. Calculated minority carrier diffusion lengths of electrons from EQE spectrum for different irradiation doses.

1
2
3
4
5
6
7
8
9
10
11
12
13
14
15
16
17
18
19
20
21
22
23
24
25
26
27
28
29
30
31
32
33
34
35
36
37
38
39
40
41
42
43
44
45
46
47
48
49
50
51
52
53
54
55
56
57
58
59
60
61
62
63
64
65

Table 5. Percentage of loss and recovery in the diffusion length of electrons calculated at 800 and 900 nm.

Dose (Gy)	Loss in Ln (%)	Recovery in Ln (%)	Loss in Ln (%)	Recovery in Ln (%)
800 nm			900 nm	
225	48	66	65	36
450	61	36	80	21
675	72	30	82	17
900	71	49	83	28

Figures 9 and 10 illustrate C–V and G/ ω –V characteristics of the cells measured under dark at room temperature, with an AC signal of 100 kHz. For the unirradiated cells, the capacitance exhibits a step-like increase in the forward bias region (0 to \sim 0.5 V), followed by a peak around 1.5 V. In the reverse bias region, the capacitance is dominated by the geometric (depletion) capacitance, as the depletion region width determines the stored charge. Conductance, on the other hand, remains negligible under reverse bias, indicating minimal carrier movement and recombination. The step in the C–V curve, observed between 0 and \sim 0.5 V, corresponds to the transition from the depletion region to the weak injection regime. In this range, the shrinking depletion width causes an increase in capacitance. As the forward bias increases further, a second peak is observed around 1.5 V, marking the transition to the high-injection regime, where minority carrier injection becomes the dominant factor. This second peak is caused by the diffusion capacitance associated with the storage of injected carriers. Beyond this point, in the very high injection regime, the capacitance decreases due to bulk transport effects. In this regime, carrier saturation and enhanced recombination occur as the injected carriers traverse the bulk of the material, leading to reduced storage capacitance. The G/ ω –V curve, in contrast, does not exhibit these distinct peaks or steps. Instead, it shows a gradual increase in conductance as the bias transitions from reverse to forward. This behavior reflects the increasing recombination and carrier transport processes as minority carriers are injected into the device. Subtle features, such as kinks or transitions, may be present in the G/ ω –V curve and could be attributed to defect-related processes or trap activation but are generally less pronounced than the peaks in the C–V curve.

After electron irradiation, the C–V and G/ ω –V curves display minimal changes in the reverse bias region, indicating that the depletion region remains largely unaffected by radiation-induced defects. However, in the forward bias regime, significant changes are evident. The step and the second peak in the C–V curve are both reduced in magnitude. This reduction is

attributed to a decrease in the efficiency of minority carrier injections, caused by enhanced recombination through radiation-induced defects. These defects act as recombination centers, suppressing the diffusion capacitance and limiting carrier storage. In the G/ω -V curve of irradiated cells, the overall conductance is lower in the forward bias region compared to unirradiated cells, consistent with reduced carrier injection and increased recombination. While the kinks or transitions in the G/ω -V curve become less distinct after irradiation, this suggests a suppression of trap-related processes due to the dominance of radiation-induced recombination. The effect of the reduced majority carrier concentration due to compensation by irradiation induced defects could also be one of the main reasons for decrease in capacitance and reduction of conductance in overall behaviors of the cells (Bhat et al., 2014; Oeba et al., 2021; Sathyanarayana Bhat et al., 2015; Yan et al., 2020; Zdravković et al., 2011)

No significant changes are observed in the C-V or G/ω -V behavior of the irradiated cells after a storage period of 52 months. This stability indicates that the radiation-induced defects remain stable over time under the given conditions, without further evolution or annealing. The persistence of the altered carrier dynamics highlights the long-term impact of electron irradiation on the electrical properties of the solar cells.

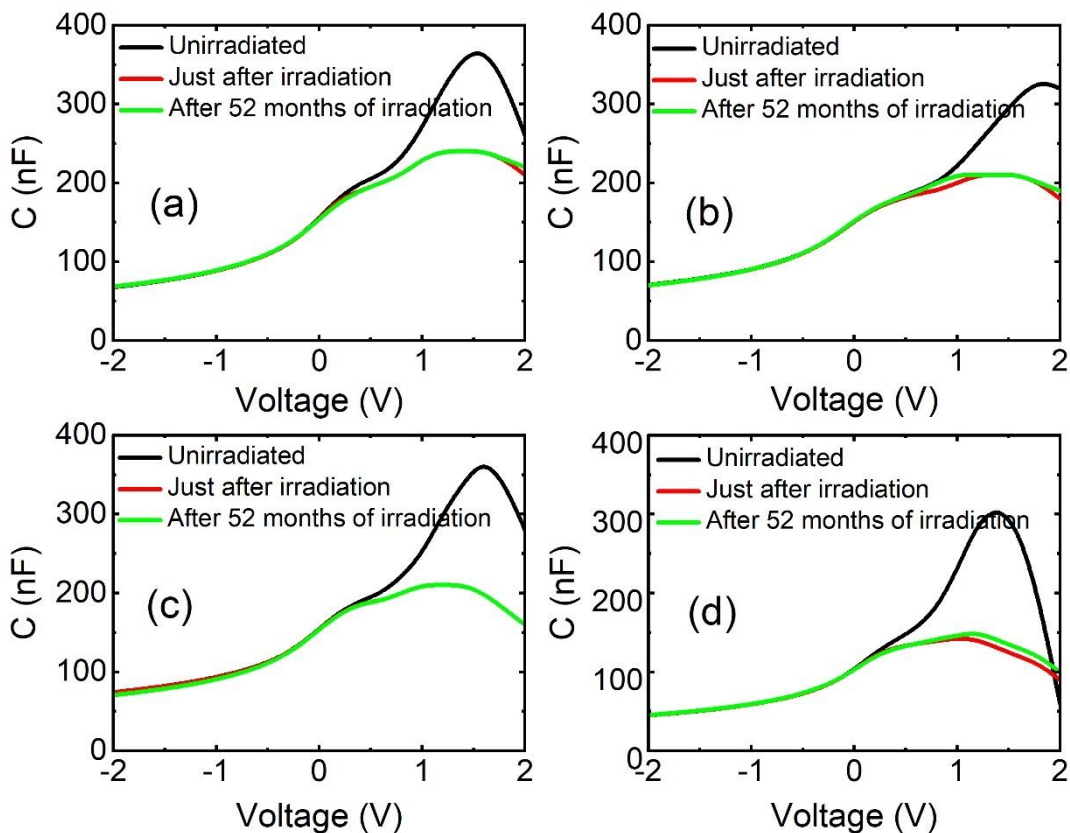


Figure 9. C-V spectrum of the cells measured under dark conditions at room temperature with an applied AC signal of 100 kHz.

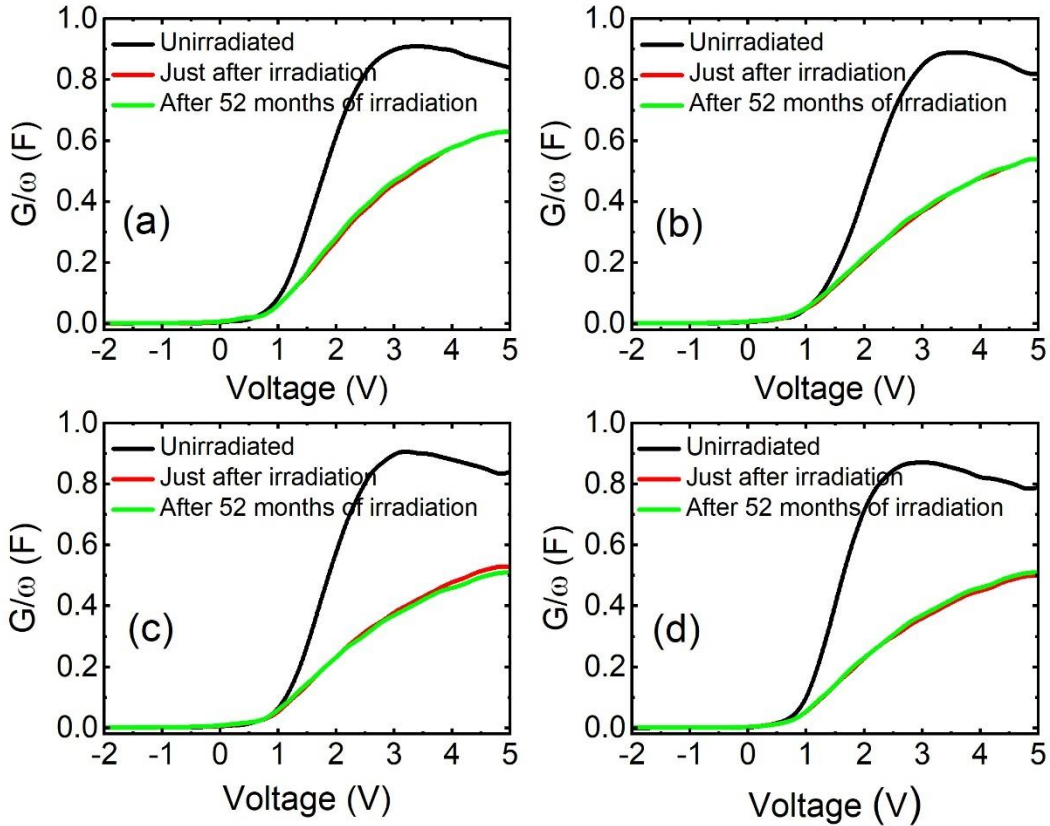


Figure 10. G-V spectrum of the cells measured under dark conditions at room temperature with an applied AC signal of 100 kHz.

4. Conclusions

This study investigated the effects of 8 MeV electron irradiation at different dose levels on c-Si solar cells and their recovery at room temperature after 52 months of irradiation. The experimental results, which compared the different doses, showed a degradation in cell parameters due to radiation-induced defects. As the electron dose level increased from the lowest to the highest dose, there was a significant reduction in efficiency values, with an efficiency loss increasing from 15% to 28%. The primary contribution to the loss of efficiency was due to a reduction in J_{SC} values, compared to moderate loss in V_{OC} . After 52 months of irradiation, a self-healing effect was observed in the devices, particularly as a remarkable recovery in the J_{SC} values. The recovery in current values was consistently verified by illuminated I-V and EQE measurements. Additionally, after 52 months of irradiation, a significant enhancement in the blue response of the cells was observed compared to the unirradiated cells, which was verified by EQE measurements. This enhancement assumed to be due to extra positive charge formation in silicon nitride film as a result oxynitrate formation in ambient atmosphere in time which could be boosted by defects formed by radiation. The

1 observed enhancement in the blue response could pave the way for new passivation approaches
2 for Si solar cells.
3
4
5

6 Acknowledgements

7 The author acknowledges the Center for Solar Energy Research and Applications (ODTÜ-
8 GÜNAM) for sample preparation and characterization and the Akdeniz University Nuclear
9 Science Research and Application Center for irradiation facility.
10
11
12
13
14

15 References

- 16 Ali, K., Khan, S.A., MatJafri, M.Z., 2016. Improved radiation resistant properties of electron
17 irradiated c-Si solar cells. *Radiation Physics and Chemistry* 125, 220–226.
18 <https://doi.org/10.1016/j.radphyschem.2016.04.015>
19
20 Ashry, M., Fares, S., 2003. Diffusion length analysis and measurement in the base region of
21 photodiodes. *Journal of Physics and Chemistry of Solids* 64, 2429–2431.
22 [https://doi.org/10.1016/S0022-3697\(03\)00285-3](https://doi.org/10.1016/S0022-3697(03)00285-3)
23
24 Babaee, S., Ghozati, S.B., 2017. The study of 1 MeV electron irradiation induced defects in
25 N-type and P-type monocrystalline silicon. *Radiation Physics and Chemistry* 141, 98–
26 102. <https://doi.org/10.1016/j.radphyschem.2017.06.012>
27
28 Basu, P.K., Singh, S.N., Arora, N.K., Chakravarty, B.C., 1994. A New Method of
29 Determination of Minority Carrier Diffusion Length in the Base Region of Silicon Solar
30 Cells, *IEEE TRANSACTIONS ON ELECTRON DEVICES*.
31
32 Bhat, P.S., Rao, A., Krishnan, S., Sanjeev, G., Puthanveettil, S.E., 2014. A study on the
33 variation of c-Si solar cell parameters under 8 MeV electron irradiation. *Solar Energy
34 Materials and Solar Cells* 120, 191–196. <https://doi.org/10.1016/j.solmat.2013.08.043>
35
36 Bhat, P.S., Rao, A., Sanjeev, G., Usha, G., Priya, G.K., Sankaran, M., Puthanveettil, S.E.,
37 2015. Capacitance and conductance studies on silicon solar cells subjected to 8MeV
38 electron irradiations. *Radiation Physics and Chemistry* 111, 28–35.
39 <https://doi.org/10.1016/j.radphyschem.2015.02.010>
40
41 Bodunrin, J.O., Moloi, S.J., 2024. Suppression of irradiation effect on electrical properties of
42 silicon diodes by iron in p-silicon. *Radiation Effects and Defects in Solids*.
43 <https://doi.org/10.1080/10420150.2024.2382269>
44
45 Bodunrin, J.O., Moloi, S.J., 2022. Current-Voltage Characteristics of 4 MeV Proton-Irradiated
46 Silicon Diodes at Room Temperature. *Silicon* 14, 10237–10244.
47 <https://doi.org/10.1007/s12633-022-01767-8>
48
49 Boztosun, I., Đapo, H., Karakoç, M., Özmen, S.F., Çeçen, Y., Çoban, A., Caner, T., Bayram,
50 E., Saito, T.R., Akdoğan, T., Bozkurt, V., Kuçuk, Y., Kaya, D., Harakeh, M.N., 2015.
51 Photonuclear reactions with zinc: A case for clinical linacs. *Eur Phys J Plus* 130, 185.
52 <https://doi.org/10.1140/epjp/i2015-15185-2>
53
54
55
56
57
58
59
60
61
62
63
64
65

- Cariou, R., Benick, J., Feldmann, F., Höhn, O., Hauser, H., Beutel, P., Razek, N.,
Wimplinger, M., Bläsi, B., Lackner, D., Hermle, M., Siefer, G., Glunz, S.W., Bett, A.W.,
Dimroth, F., 2018. III-V-on-silicon solar cells reaching 33% photoconversion efficiency
in two-terminal configuration. *Nat Energy* 3, 326–333. <https://doi.org/10.1038/s41560-018-0125-0>
- Danilchenko, B., Budnyk, A., Shpinar, L., Poplavskyy, D., Zelensky, S.E., Barnham, K.W.J.,
Ekins-Daukes, N.J., 2008. 1 MeV electron irradiation influence on GaAs solar cell
performance. *Solar Energy Materials and Solar Cells* 92, 1336–1340.
<https://doi.org/10.1016/j.solmat.2008.05.006>
- Es, F., Kulakci, M., Turan, R., 2016. An Alternative Metal-Assisted Etching Route for
Texturing Silicon Wafers for Solar Cell Applications. *IEEE J Photovolt* 6, 440–446.
<https://doi.org/10.1109/JPHOTOV.2016.2520207>
- Essig, S., Allebé, C., Remo, T., Geisz, J.F., Steiner, M.A., Horowitz, K., Barraud, L., Ward,
J.S., Schnabel, M., Descoeuilles, A., Young, D.L., Woodhouse, M., Despeisse, M.,
Ballif, C., Tamboli, A., 2017. Raising the one-sun conversion efficiency of III-V/Si solar
cells to 32.8% for two junctions and 35.9% for three junctions. *Nat Energy* 2, 17144.
<https://doi.org/10.1038/nenergy.2017.144>
- Essig, S., Steiner, M.A., Allebé, C., Geisz, J.F., Paviet-Salomon, B., Ward, S., Descoeuilles,
A., LaSalvia, V., Barraud, L., Badel, N., Faes, A., Levrat, J., Despeisse, M., Ballif, C.,
Stradins, P., Young, D.L., 2016. Realization of GaInP/Si Dual-Junction Solar Cells with
29.8% 1-Sun Efficiency. *IEEE J Photovolt* 6, 1012–1019.
<https://doi.org/10.1109/JPHOTOV.2016.2549746>
- Feklisova, O. V., Yarykin, N.A., Weber, J., 2013. Annealing kinetics of boron-containing
centers in electron-irradiated silicon. *Semiconductors* 47, 228–231.
<https://doi.org/10.1134/S1063782613020085>
- Giesecke, J.A., Michl, B., Schindler, F., Schubert, M.C., Warta, W., 2011. Minority carrier
lifetime of silicon solar cells from quasi-steady-state photoluminescence. *Solar Energy
Materials and Solar Cells* 95, 1979–1982. <https://doi.org/10.1016/j.solmat.2011.02.023>
- Green, M.A., 2016. Commercial progress and challenges for photovoltaics. *Nat Energy* 1,
15015. <https://doi.org/10.1038/nenergy.2015.15>
- Hamache, A., Sengouga, N., Meftah, A., Henini, M., 2016. Modeling the effect of 1 MeV
electron irradiation on the performance of n+-p-p+ silicon space solar cells. *Radiation
Physics and Chemistry* 123, 103–108.
<https://doi.org/10.1016/j.radphyschem.2016.02.025>
- Hisamatsu, T., Kawasaki, O., Matsuda, S., Nakao, T., Wakow, Y., 1998. Radiation
degradation of large fluence irradiated space silicon solar cells. *Solar Energy Materials
and Solar Cells* 50, 331–338. [https://doi.org/10.1016/S0927-0248\(97\)00163-3](https://doi.org/10.1016/S0927-0248(97)00163-3)
- Honsberg, C., Bowden, S., 2019. Generation Rate [WWW Document]. URL
<https://www.pveducation.org/pvcdrom/pn-junctions/generation-rate> (accessed 1.19.25).

- Horiuchi, N., Nozaki, T., Chiba, A., 2000. Improvement in electrical performance of
radiation-damaged silicon solar cells by annealing. Nucl Instrum Methods Phys Res A
443, 186–193. [https://doi.org/10.1016/S0168-9002\(99\)01013-X](https://doi.org/10.1016/S0168-9002(99)01013-X)
- Imaizumi, M., Taylor, S.J., Yamaguchi, M., Ito, T., Hisamatsu, T., Matsuda, S., 1999.
Analysis of structure change of Si solar cells irradiated with high fluence electrons.
- Jasenek, A., Rau, U., 2001. Defect generation in Cu(In,Ga)Se₂ heterojunction solar cells by
high-energy electron and proton irradiation. J Appl Phys 90, 650–658.
<https://doi.org/10.1063/1.1379348>
- Junga, F.A., Enslow, G.M., 1959. Radiation Effects in Silicon Solar Cells. IRE Transactions
on Nuclear Science 6, 49–53. <https://doi.org/10.1109/TNS2.1959.4315679>
- Kabaçelik, İ., 2023. Investigation of the Effect of Successive Low-Dose γ -Rays on c-Si Solar
Cell. Gazi Üniversitesi Fen Bilimleri Dergisi Part C: Tasarım ve Teknoloji 11, 582–591.
<https://doi.org/10.29109/gujsc.1199922>
- Kabacelik, I., Kutaruk, H., Yalatkaya, S., Sahin, R., 2017. γ irradiation induced effects on the
TCO thin films. Radiation Physics and Chemistry 134, 89–92.
<https://doi.org/10.1016/j.radphyschem.2017.01.042>
- Kawakita, S., Imaizumi, M., Yamaguchi, M., Kushiya, K., Ohshima, T., Itoh, H., Matsuda, S.,
2002. Annealing enhancement effect by light illumination on proton irradiated
Cu(In,Ga)Se₂ thin-film solar cells. Jpn J Appl Phys 41, L797–L799.
<https://doi.org/10.1143/jjap.41.l797>
- Khan, A., Yamaguchi, M., Ohshita, Y., Dharmaraso, N., Araki, K., Khanh, V.T., Itoh, H.,
Ohshima, T., Imaizumi, M., Matsuda, S., 2003. Strategies for improving radiation
tolerance of Si space solar cells, Solar Energy Materials & Solar Cells.
- Krishnan, S., Sanjeev, G., Pattabi, M., 2007. 8 MeV electron irradiation effects in silicon
photo-detectors. Nucl Instrum Methods Phys Res B 264, 79–82.
<https://doi.org/10.1016/j.nimb.2007.08.004>
- Krishnan, S., Sanjeev, G., Pattabi, M., Mathew, X., 2009. Effect of electron irradiation on the
properties of CdTe/CdS solar cells. Solar Energy Materials and Solar Cells 93, 2–5.
<https://doi.org/10.1016/j.solmat.2007.12.002>
- Kuendig, J., Goetz, M., Shah, A., Gerlach, L., Fernandez, E., 2003. Thin film silicon solar
cells for space applications: Study of proton irradiation and thermal annealing effects on
the characteristics of solar cells and individual layers. Solar Energy Materials and Solar
Cells 79, 425–438. [https://doi.org/10.1016/S0927-0248\(02\)00486-5](https://doi.org/10.1016/S0927-0248(02)00486-5)
- Kulakci, M., Es, F., Ozdemir, B., Unalan, H.E., Turan, R., 2013. Application of si nanowires
fabricated by metal-assisted etching to crystalline si solar cells. IEEE J Photovolt 3, 548–
553. <https://doi.org/10.1109/JPHOTOV.2012.2228300>
- Lang, F., Nickel, N.H., Bundesmann, J., Seidel, S., Denker, A., Albrecht, S., Brus, V. V.,
Rappich, J., Rech, B., Landi, G., Neitzert, H.C., 2016. Radiation Hardness and Self-
Healing of Perovskite Solar Cells. Advanced Materials 28, 8726–8731.
<https://doi.org/10.1002/adma.201603326>

- Leguijt, C., Lislegen, P., Eikelboom, J.A., Weeber, A.W., Schuurmans, F.M., Sinke, W.C.,
Alkemade, P.F.A., Sarro, P.M., Marte, C.H.M., Verhoef, L.A., 1996. Low temperature
surface passivation for silicon solar cells, / Solar Energy Materials and Solar Cells.
- Lelièvre, J.-F, Fourmond, E., Kaminski, A., Palais, Olivier, Ballutaud, D., Lemiti, M.,
Lelièvre, J-F, Palais, O, 2009. Study of the composition of hydrogenated silicon nitride
SiNx:H for efficient surface and bulk passivation of silicon. Solar Energy Materials and
Solar Cells 93. <https://doi.org/10.1016/j.solmat.2009.01.023>
- Li, J., Aierken, A., Liu, Y., Zhuang, Y., Yang, X., Mo, J.H., Fan, R.K., Chen, Q.Y., Zhang,
S.Y., Huang, Y.M., Zhang, Q., 2021. A Brief Review of High Efficiency III-V Solar
Cells for Space Application. Front Phys. <https://doi.org/10.3389/fphy.2020.631925>
- Li, P., Dong, H., Lan, J., Bai, Y., He, C., Ma, L., Li, Y., Liu, J., 2022. Tolerance of Perovskite
Solar Cells under Proton and Electron Irradiation. Materials 15.
<https://doi.org/10.3390/ma15041393>
- Liao, C., Fretwurst, E., Garutti, E., Schwandt, J., Makarenko, L., Pintilie, I., Filip, L.D.,
Himmerlich, A., Moll, M., Gurimskaya, Y., Li, Z., 2023. Investigation of the Boron
removal effect induced by 5.5MeV electrons on highly doped EPI- and Cz-silicon. Nucl
Instrum Methods Phys Res A 1056. <https://doi.org/10.1016/j.nima.2023.168559>
- Luft, W., 1964. Effects of Electron Irradiation on N on P Silicon Solar Cells. IEEE
Transactions on Aerospace 2, 747–758. <https://doi.org/10.1109/TA.1964.4319662>
- Matsuura, H., Iwata, H., Kagamihara, S., Ishihara, R., Komeda, M., Imai, H., Kikuta, M.,
Inoue, Y., Hisamatsu, T., Kawakita, S., Ohshima, T., Itoh, H., 2006. Si substrate suitable
for radiation-resistant space solar cells. Jpn J Appl Phys 45, 2648–2655.
<https://doi.org/10.1143/JJAP.45.2648>
- Medjoubi, K., Lefèvre, J., Vauche, L., Veinberg-Vidal, E., Jany, C., Rostaing, C., Amalbert,
V., Chabuel, F., Boizot, B., Cariou, R., 2021. Electrons irradiation of III-V//Si solar cells
for NIRT conditions. Solar Energy Materials and Solar Cells 223, 110975.
<https://doi.org/10.1016/j.solmat.2021.110975>
- Mizuno, H., Makita, K., Sai, H., Mochizuki, T., Matsui, T., Takato, H., Müller, R., Lackner,
D., Dimroth, F., Sugaya, T., 2022. Integration of Si Heterojunction Solar Cells with III-V
Solar Cells by the Pd Nanoparticle Array-Mediated “Smart Stack” Approach. ACS Appl
Mater Interfaces 14, 11322–11329. <https://doi.org/10.1021/acsami.1c22458>
- Morita, Y., Ohshima, T., Nashiyama, I., Yamamoto, Y., Kawasaki, O., Matsuda, S., 1997.
Anomalous degradation in silicon solar cells subjected to high-fluence proton and
electron irradiations. J Appl Phys 81, 6491–6493. <https://doi.org/10.1063/1.364437>
- Nikolić, D., Stanković, K., Timotijević, L., Rajović, Z., Vujisić, M., 2013. Comparative study
of gamma radiation effects on solar cells, photodiodes, and phototransistors.
International Journal of Photoenergy 2013, 843174. <https://doi.org/10.1155/2013/843174>
- Nikolić, D., Vasić-Milovanović, A., Obrenović, M., Doličanin, E., 2015. Effects of successive
gamma and neutron irradiation on solar cells. Journal of Optoelectronics and Advanced
Materials 17, 351–356.

- Oeba, D.A., Bodunrin, J.O., Moloi, S.J., 2024. Enhancing radiation-hardness of Si-based diodes: An investigation of Al-doping effects in Si using I–V measurements. *Radiation Physics and Chemistry* 223. <https://doi.org/10.1016/j.radphyschem.2024.111873>
- Oeba, D.A., Bodunrin, J.O., Moloi, S.J., 2021. Electrical properties of 3 MeV proton irradiated silicon Schottky diodes. *Physica B Condens Matter* 610. <https://doi.org/10.1016/j.physb.2020.412786>
- Onoda, S., Hirao, T., Laird, J.S., Mori, H., Okamoto, T., Koizumi, Y., Itoh, H., 2002. Spectral response of a gamma and electron irradiated pin photodiode. *IEEE Trans Nucl Sci* 49 III, 1446–1449. <https://doi.org/10.1109/TNS.2002.1039681>
- Pellegrino, C., Gagliardi, A., Zimmermann, C.G., 2019. Difference in space-charge recombination of proton and electron irradiated GaAs solar cells. *Progress in Photovoltaics: Research and Applications* 27, 379–390. <https://doi.org/10.1002/pip.3100>
- Radu, R., Fretwurst, E., Klanner, R., Lindstroem, G., Pintilie, I., 2013. Radiation damage in n-type silicon diodes after electron irradiation with energies between 1.5 MeV and 15 MeV. *Nucl Instrum Methods Phys Res A* 730, 84–90. <https://doi.org/10.1016/j.nima.2013.04.080>
- Raider, S.I., Flitsch, R., Aboaf, J.A., Pliskin, W.A., n.d. Surface Oxidation of Silicon Nitride Films. *J Electrochem Soc* 123, 560–565. <https://doi.org/10.1149/1.2132877>
- Raya-Armenta, J.M., Bazmohammadi, N., Vasquez, J.C., Guerrero, J.M., 2021. A short review of radiation-induced degradation of III–V photovoltaic cells for space applications. *Solar Energy Materials and Solar Cells*. <https://doi.org/10.1016/j.solmat.2021.111379>
- Robertson, J., 1993. Electronic Structure of Defects in Amorphous Silicon Nitride. *MRS Online Proceedings Library* 284, 65–76. <https://doi.org/https://doi.org/10.1557/PROC-284-65>
- Saad, A.M., 2002. Effect of cobalt 60 and 1 MeV electron irradiation on silicon photodiodes/solar cells. *Can J Phys* 80, 1591–1599. <https://doi.org/10.1139/p02-037>
- Sahin, R., Kabacelik, I., 2018. Effects of ionizing radiation on the properties of monocrystalline Si solar cells. *Radiation Physics and Chemistry* 150, 90–94. <https://doi.org/10.1016/j.radphyschem.2018.04.033>
- Sathyanarayana Bhat, P., Rao, A., Sanjeev, G., Usha, G., Priya, G.K., Sankaran, M., Puthanveettil, S.E., 2015. Capacitance and conductance studies on silicon solar cells subjected to 8MeV electron irradiations. *Radiation Physics and Chemistry* 111, 28–35. <https://doi.org/10.1016/j.radphyschem.2015.02.010>
- Sato, S. ichiro, Miyamoto, H., Imaizumi, M., Shimazaki, K., Morioka, C., Kawano, K., Ohshima, T., 2009. Degradation modeling of InGaP/GaAs/Ge triple-junction solar cells irradiated with various-energy protons. *Solar Energy Materials and Solar Cells* 93, 768–773. <https://doi.org/10.1016/j.solmat.2008.09.044>

- Schmidt, J., Aberle, A.G., 1999. Carrier recombination at silicon-silicon nitride interfaces fabricated by plasma-enhanced chemical vapor deposition. *J Appl Phys* 85, 3626–3633. <https://doi.org/10.1063/1.369725>
- Schnabel, M., Schulte-Huxel, H., Rienäcker, M., Warren, E.L., Ndione, P.F., Nemeth, B., Klein, T.R., Van Hest, M.F.A.M., Geisz, J.F., Peibst, R., Stradins, P., Tamboli, A.C., 2020. Three-terminal III-V/Si tandem solar cells enabled by a transparent conductive adhesive. *Sustain Energy Fuels* 4, 549–558. <https://doi.org/10.1039/c9se00893d>
- Schygulla, P., Müller, R., Lackner, D., Höhn, O., Hauser, H., Bläsi, B., Predan, F., Benick, J., Hermle, M., Glunz, S.W., Dimroth, F., 2022. Two-terminal III-V//Si triple-junction solar cell with power conversion efficiency of 35.9 % at AM1.5g. *Progress in Photovoltaics: Research and Applications* 30, 869–879. <https://doi.org/10.1002/pip.3503>
- Sharma, D., Mehra, R., Raj, B., 2022. Methods for Integration of III-V Compound and Silicon Multijunction for High Efficiency Solar Cell Design. *Silicon* 14, 9797–9804. <https://doi.org/10.1007/s12633-022-01691-x>
- Sharma, V., Tracy, C., Schroder, D., Flores, M., Dauksher, B., Bowden, S., 2013. Study and manipulation of charges present in silicon nitride films, in: Conference Record of the IEEE Photovoltaic Specialists Conference. Institute of Electrical and Electronics Engineers Inc., pp. 1288–1293. <https://doi.org/10.1109/PVSC.2013.6744377>
- Shen, X.B., Aierken, A., Heini, M., Mo, J.H., Lei, Q.Q., Zhao, X.F., Sailai, M., Xu, Y., Tan, M., Wu, Y.Y., Lu, S.L., Li, Y.D., Guo, Q., 2019. Degradation analysis of 1 MeV electron and 3 MeV proton irradiated InGaAs single junction solar cell. *AIP Adv* 9, 075205. <https://doi.org/10.1063/1.5094472>
- Srour, J.R., Marshall, C.J., Marshall, P.W., 2003. Review of displacement damage effects in silicon devices. *IEEE Trans Nucl Sci* 50, 653–670. <https://doi.org/10.1109/TNS.2003.813197>
- Summers, G.P., Burke, E.A., Xapsos, M.A., 1995. Displacement damage analogs to ionizing radiation effects. *Radiat Meas* 24, 1–8. [https://doi.org/10.1016/1350-4487\(94\)00093-G](https://doi.org/10.1016/1350-4487(94)00093-G)
- Taylor, S.J., Yamaguchi, M., Yang, M.J., Imaizumi, M., Matsuda, S., Kawasaki, O., Hisamatsu, T., 1997. Type conversion in irradiated silicon diodes. *Appl Phys Lett* 70, 2165–2167. <https://doi.org/10.1063/1.118946>
- Tobnaghi, D.M., Rahnamaei, A., Vajdi, M., 2014. Experimental Study of Gamma Radiation Effects on the Electrical Characteristics of Silicon Solar Cells. *Int. J. Electrochem. Sci.* 9, 2824–2831.
- Verduci, R., Romano, V., Brunetti, G., Yaghoobi Nia, N., Di Carlo, A., D'Angelo, G., Ciminelli, C., 2022. Solar Energy in Space Applications: Review and Technology Perspectives. *Adv Energy Mater* 12, 2200125. <https://doi.org/10.1002/aenm.202200125>
- Weiss, C., Park, S., Lefèvre, J., Boizot, B., Mohr, C., Cavani, O., Picard, S., Kurstjens, R., Niewelt, T., Janz, S., 2020. Electron and proton irradiation effect on the minority carrier lifetime in SiC passivated p-doped Ge wafers for space photovoltaics. *Solar Energy Materials and Solar Cells* 209, 110430. <https://doi.org/10.1016/j.solmat.2020.110430>

Yamaguchi, M., 2001. Radiation-resistant solar cells for space use. *Solar Energy Materials and Solar Cells* 68, 31–53. [https://doi.org/https://doi.org/10.1016/S0927-0248\(00\)00344-5](https://doi.org/10.1016/S0927-0248(00)00344-5)

Yamaguchi, M., Khan, A., Taylor, S.J., Ando, K., Yamaguchi, T., Matsuda, S., Aburaya, T., 1999. Deep level analysis of radiation-induced defects in Si crystals and solar cells.

Yamaguchi, M., Taylor, S.J., Matsuda, S., Kawasaki, O., Ando, K., 1996. Analysis of damage to silicon solar cells by high fluence electron irradiation, in: Conference Record of the IEEE Photovoltaic Specialists Conference. IEEE, pp. 167–170. <https://doi.org/10.1109/pvsc.1996.563973>

Yan, G., Wang, J. ling, Liu, J., Liu, Y. yu, Wu, R., Wang, R., 2020. Electroluminescence analysis of VOC degradation of individual subcell in GaInP/GaAs/Ge space solar cells irradiated by 1.0 MeV electrons. *J Lumin* 219, 116905. <https://doi.org/10.1016/j.jlumin.2019.116905>

Yang, J., Bao, Q., Shen, L., Ding, L., 2020. Potential applications for perovskite solar cells in space. *Nano Energy* 76, 105019. <https://doi.org/10.1016/j.nanoen.2020.105019>

Yang, S.-S., Gao, X., Wang, Y.-F., Feng, Z.-Z., 2011. Displacement Damage Characterization of Electron Radiation in Triple-Junction GaAs Solar Cells. *J Spacecr Rockets* 48, 23–26. <https://doi.org/10.2514/1.48873>

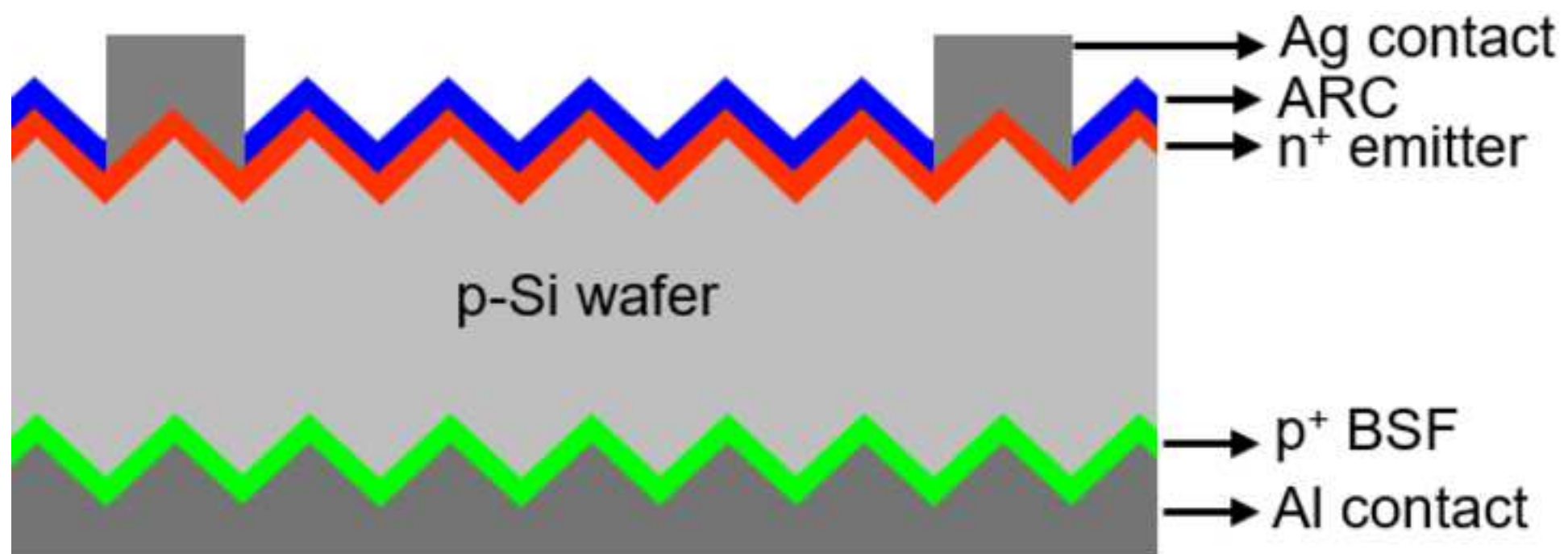
Yu, S., Rabelo, M., Yi, J., 2022. A Brief Review on III-V/Si Tandem Solar Cells. *Transactions on Electrical and Electronic Materials*. <https://doi.org/10.1007/s42341-022-00398-5>

Zdravković, M.R., Vasić, A.I., Radosavljević, R.L., Vujišić, M.L., Osmokrović, P. V., 2011. Influence of radiation on the properties of solar cells. *Nuclear Technology and Radiation Protection* 26, 158–163. <https://doi.org/10.2298/NTRP1102158Z>

Zh Karazhanov, S., 2000. Effect of radiation-induced defects on silicon solar cells. *J Appl Phys* 88, 3941–3947. <https://doi.org/https://doi.org/10.1063/1.1290453>

Zhang, Y., Qi, C., Wang, T., Ma, G., Tsai, H.S., Liu, C., Zhou, J., Wei, Y., Li, H., Xiao, L., Ma, Y., Wang, D., Tang, C., Li, J., Wu, Z., Huo, M., 2020. Electron Irradiation Effects and Defects Analysis of the Inverted Metamorphic Four-Junction Solar Cells. *IEEE J Photovolt* 10, 1712–1720. <https://doi.org/10.1109/JPHOTOV.2020.3025442>

Zhang, Y., Zhang, H., Yu, B., Wang, W., Hou, R., Chen, B., Xu, Q., Zhou, Y., Qin, G., 2014. Gamma-ray irradiation hardness of arrayed silicon microhole-based radial p-n junction solar cells. *J Phys D Appl Phys* 47, 065101. <https://doi.org/10.1088/0022-3727/47/6/065101>



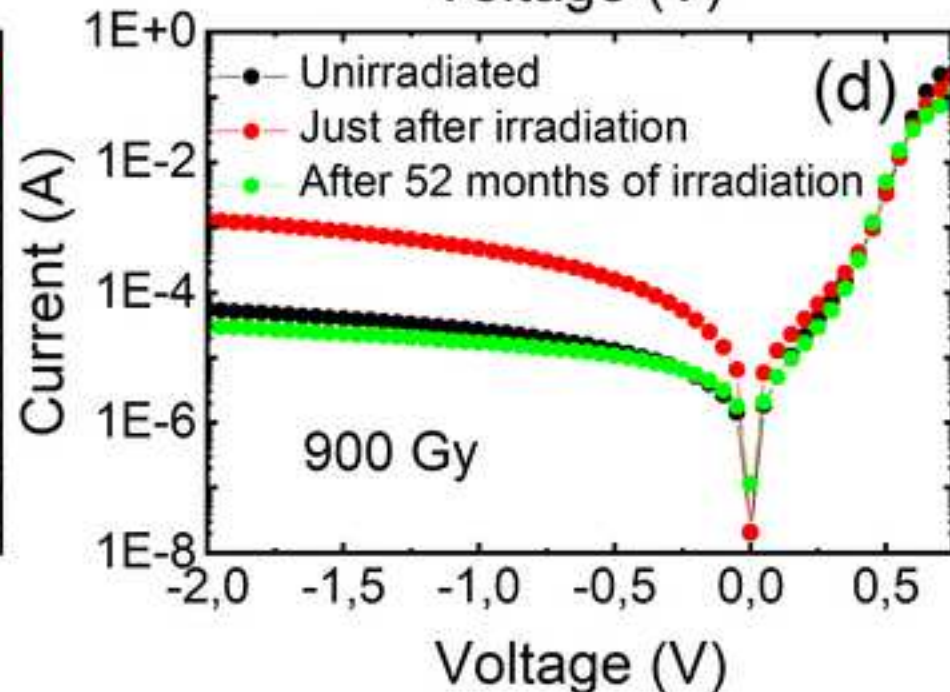
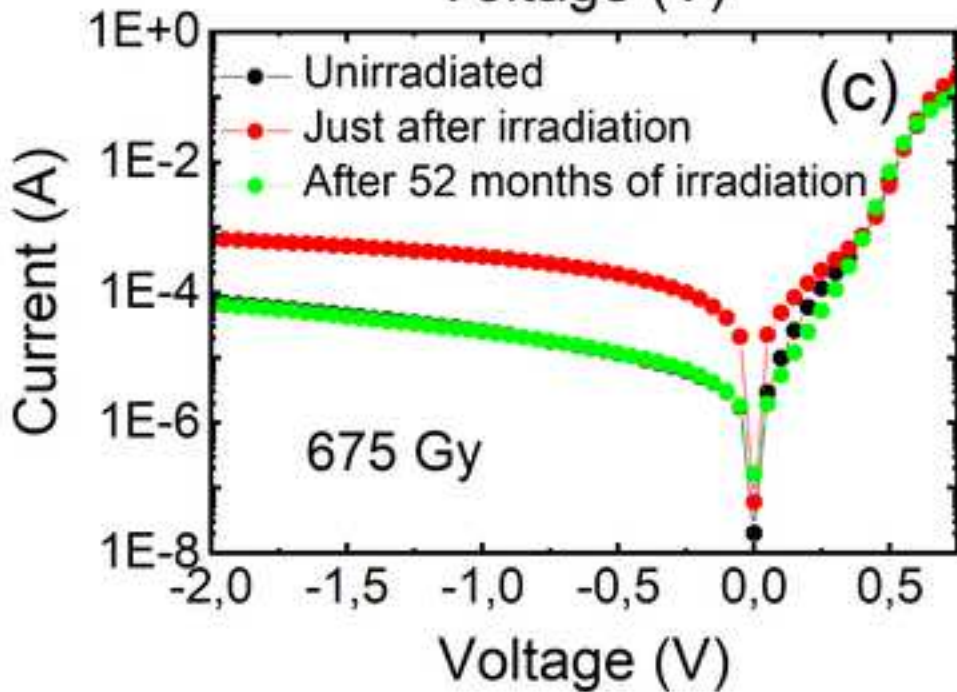
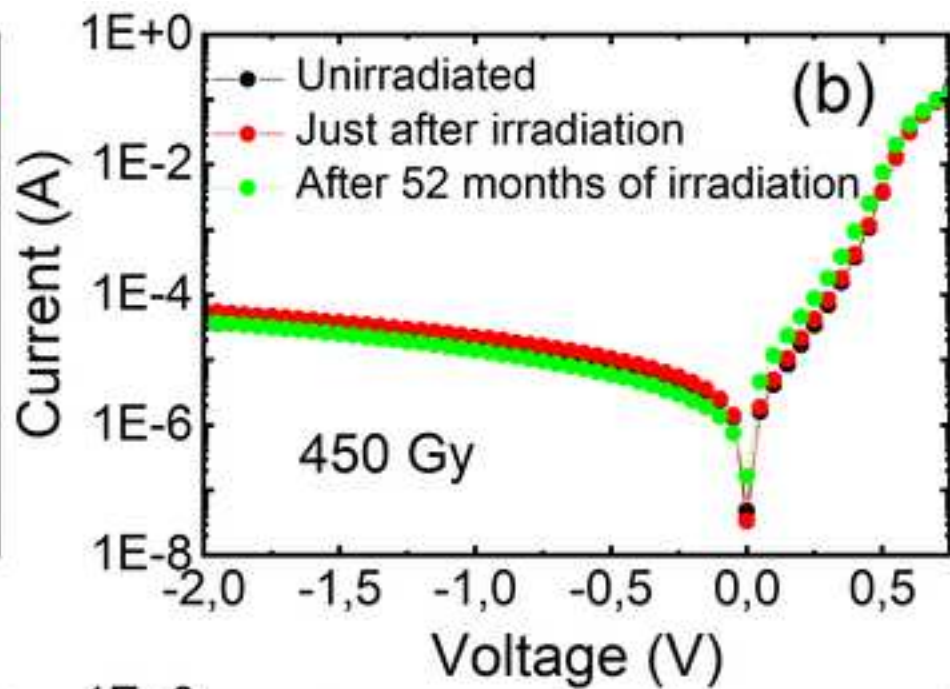
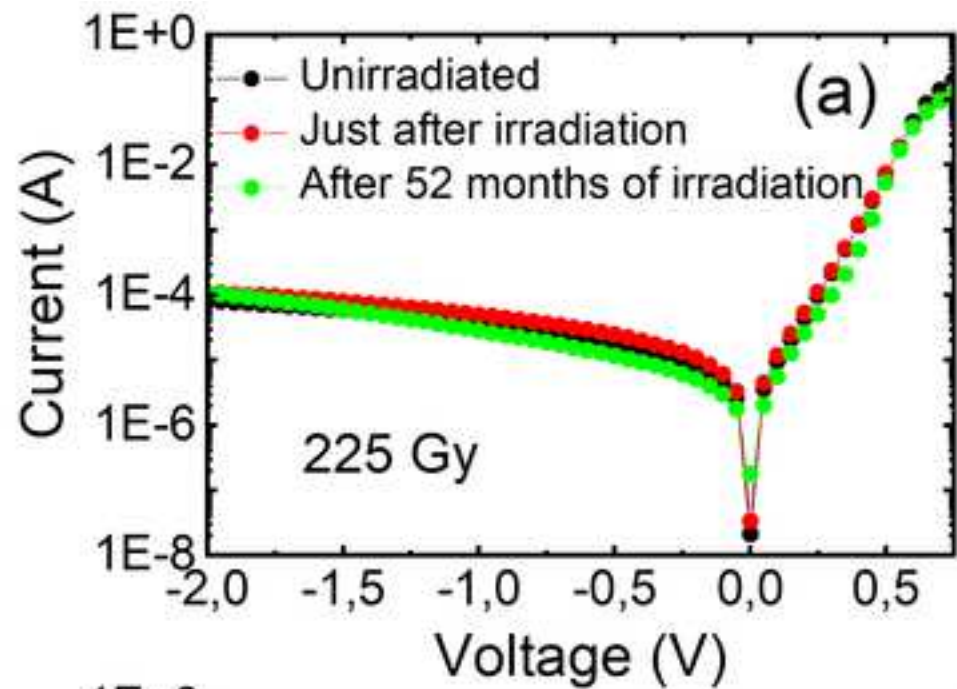


Figure 3

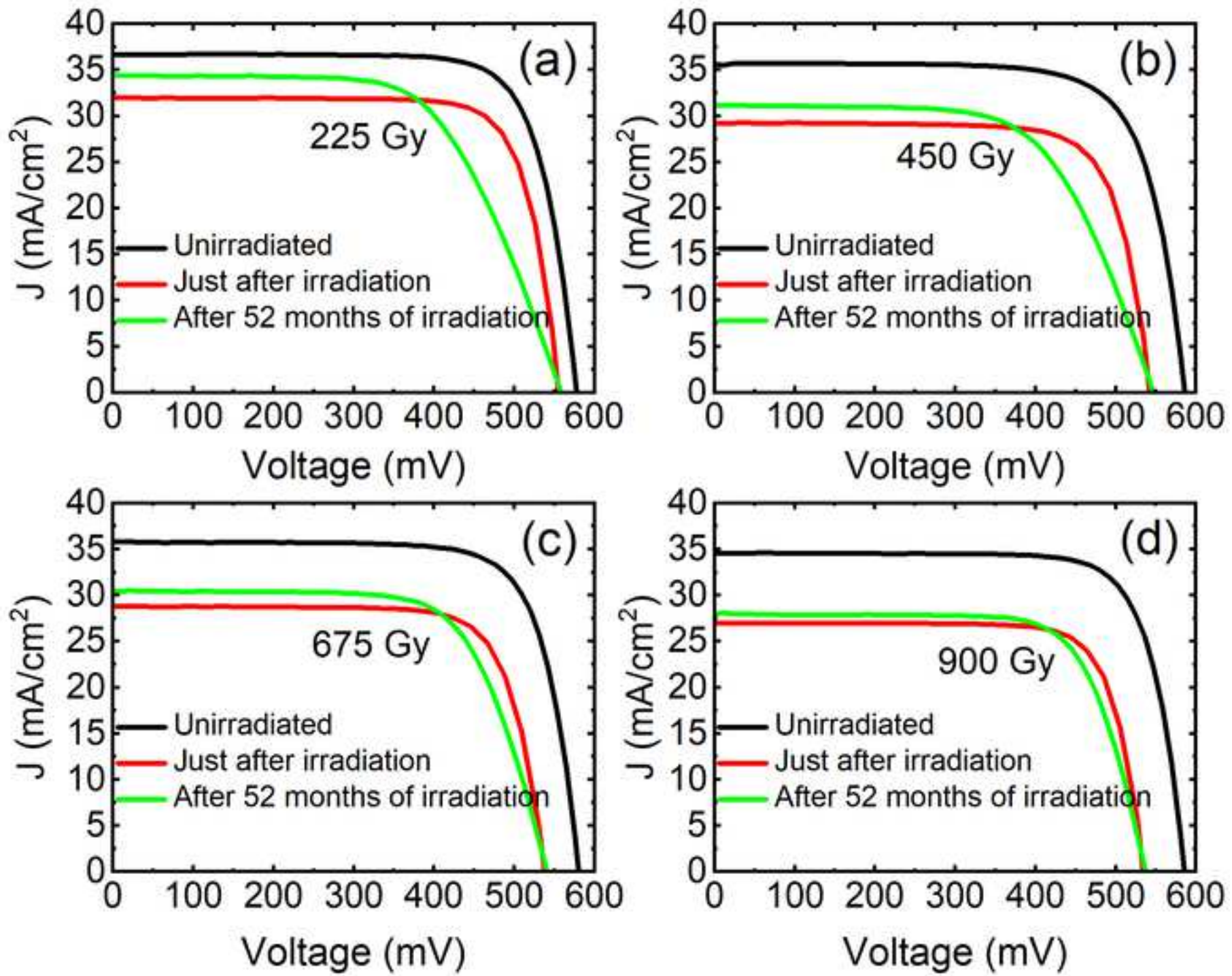
[Click here to access/download;Figure;Figure 3.jpg](#)

Figure 4a

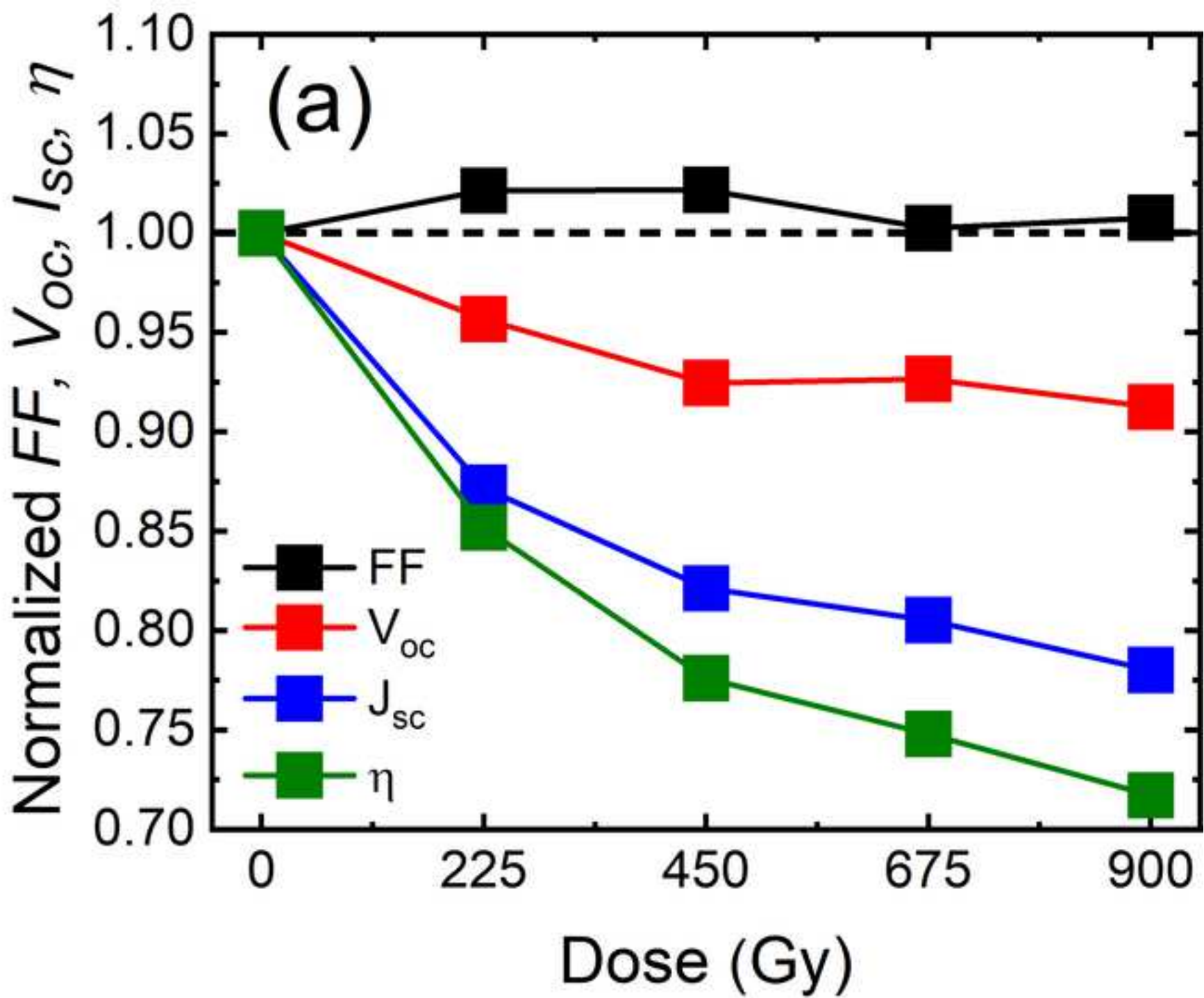
[Click here to access/download;Figure;Figure 4a.jpg](#)

Figure 4b

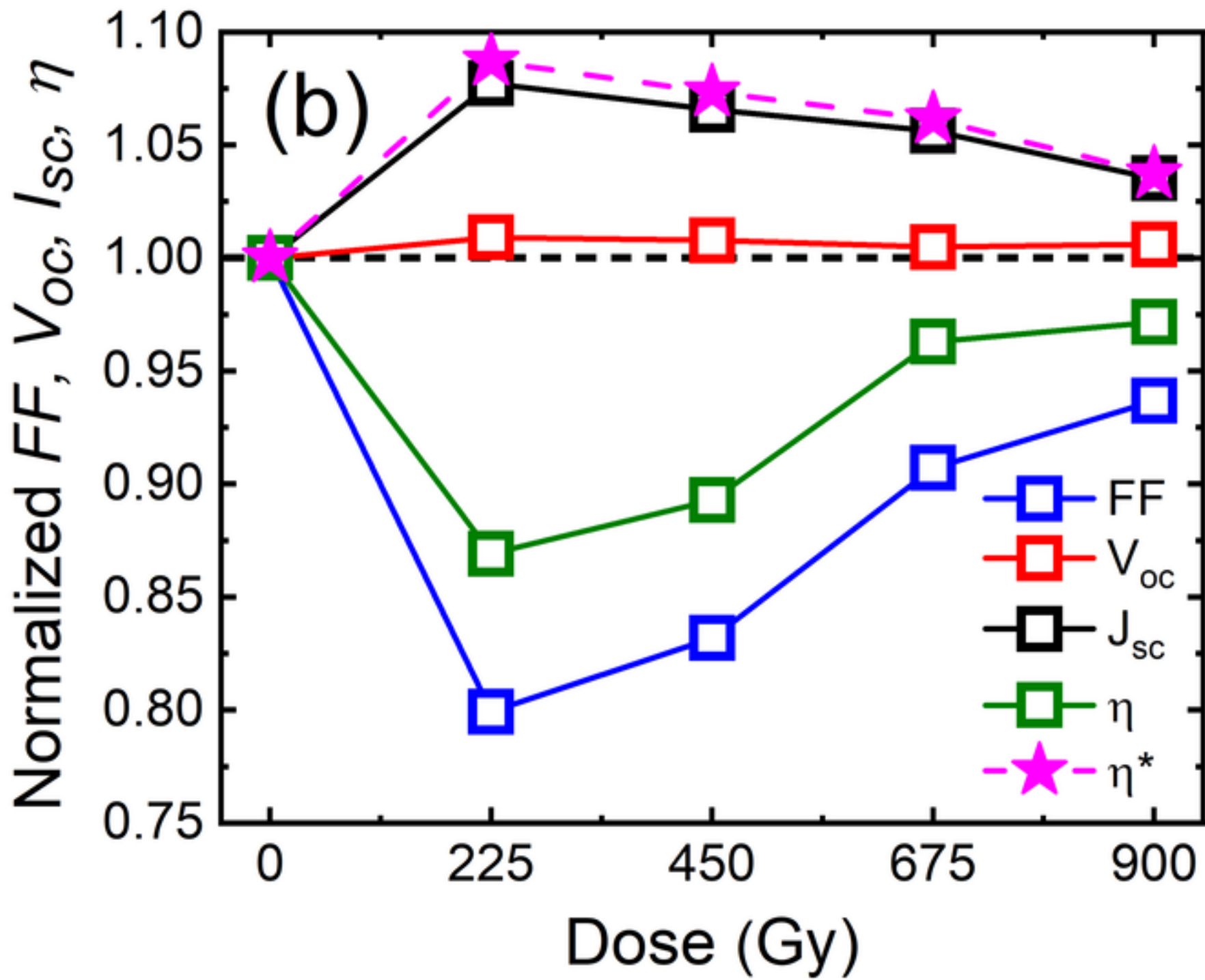
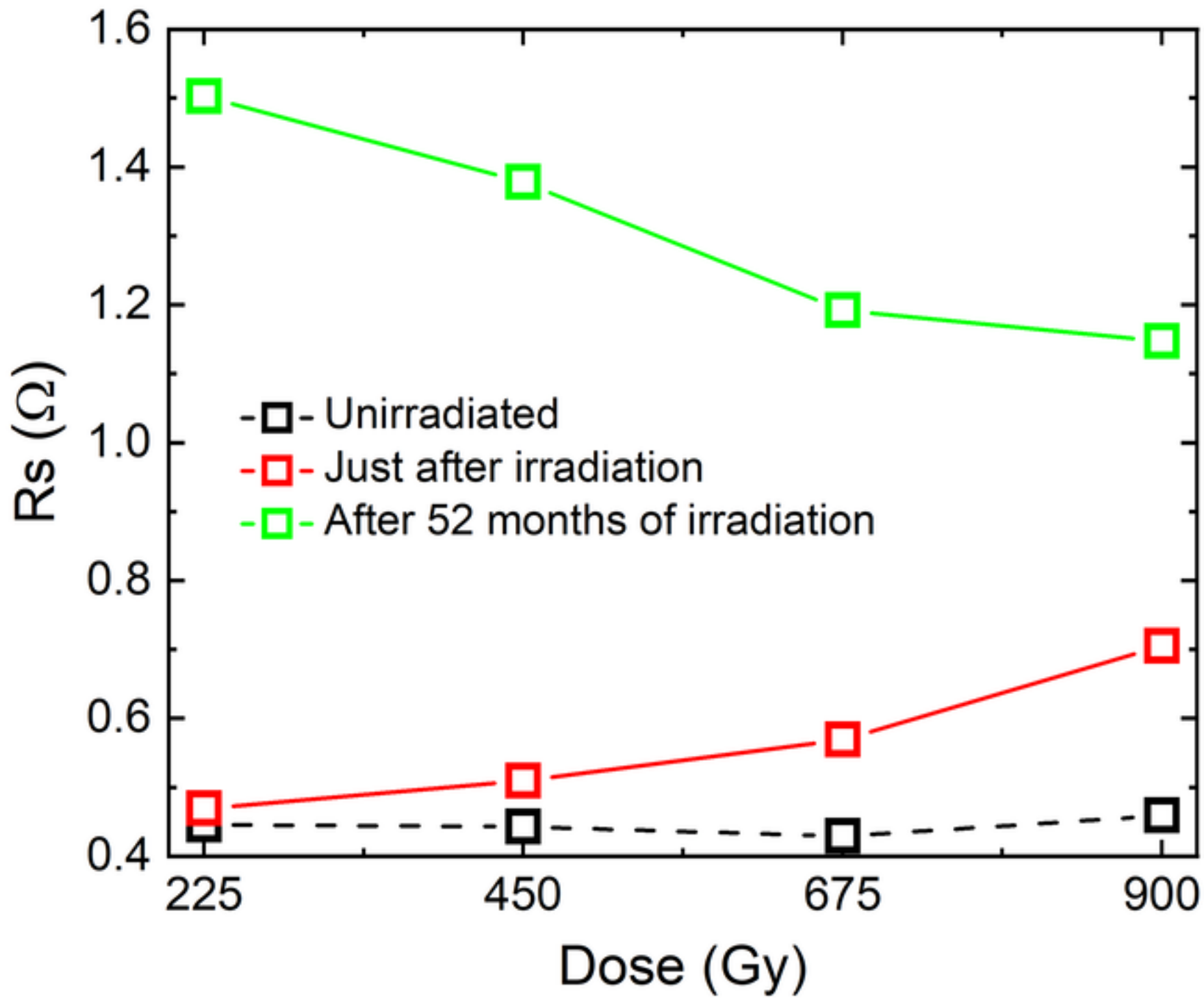
[Click here to access/download;Figure;Figure 4b.jpg](#)

Figure 5

[Click here to access/download;Figure;Figure 5.jpg](#)

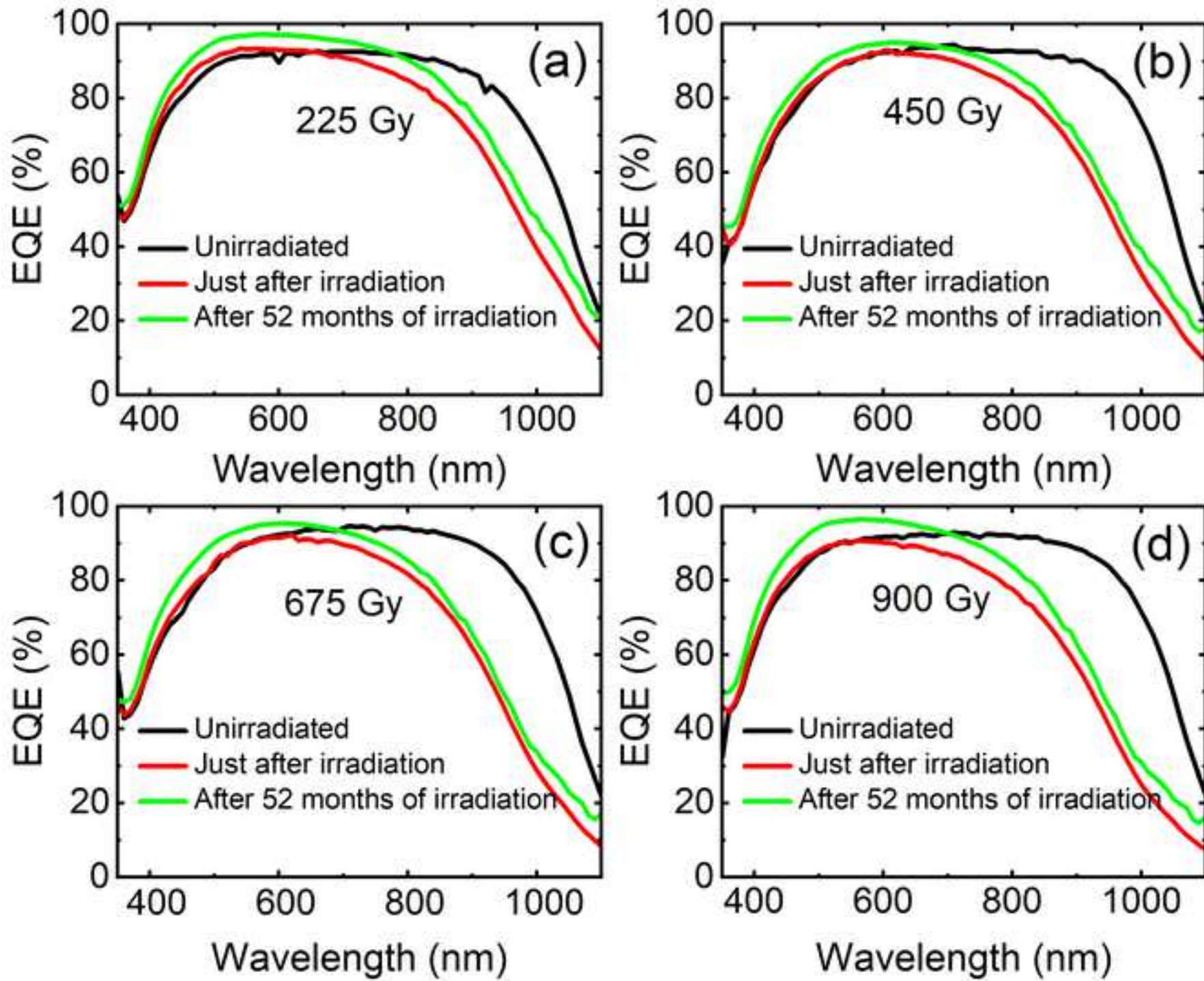


Figure 7

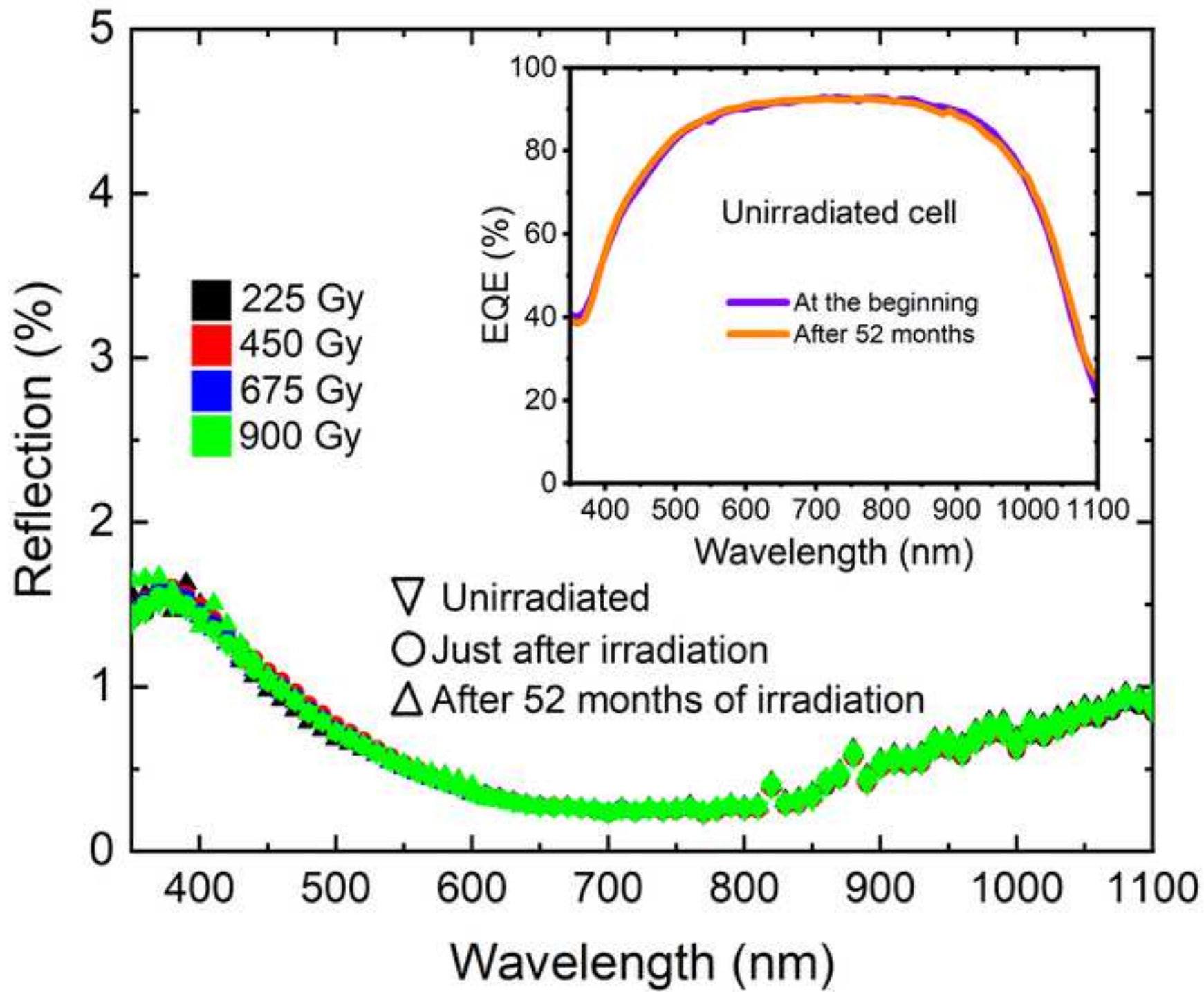
[Click here to access/download;Figure;Figure 7.jpg](#)

Figure 8

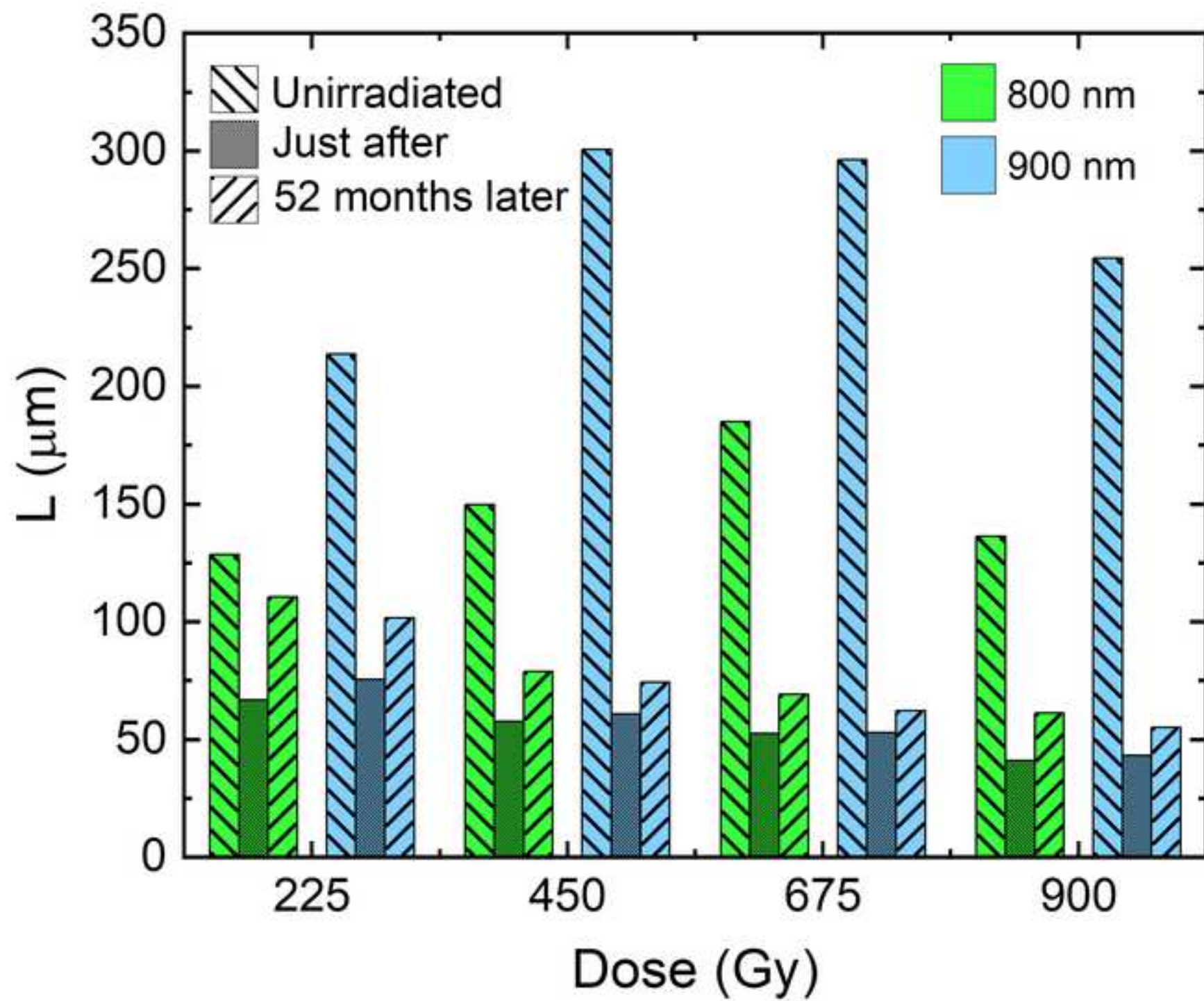
[Click here to access/download;Figure;Figure 8.jpg](#)

Figure 9

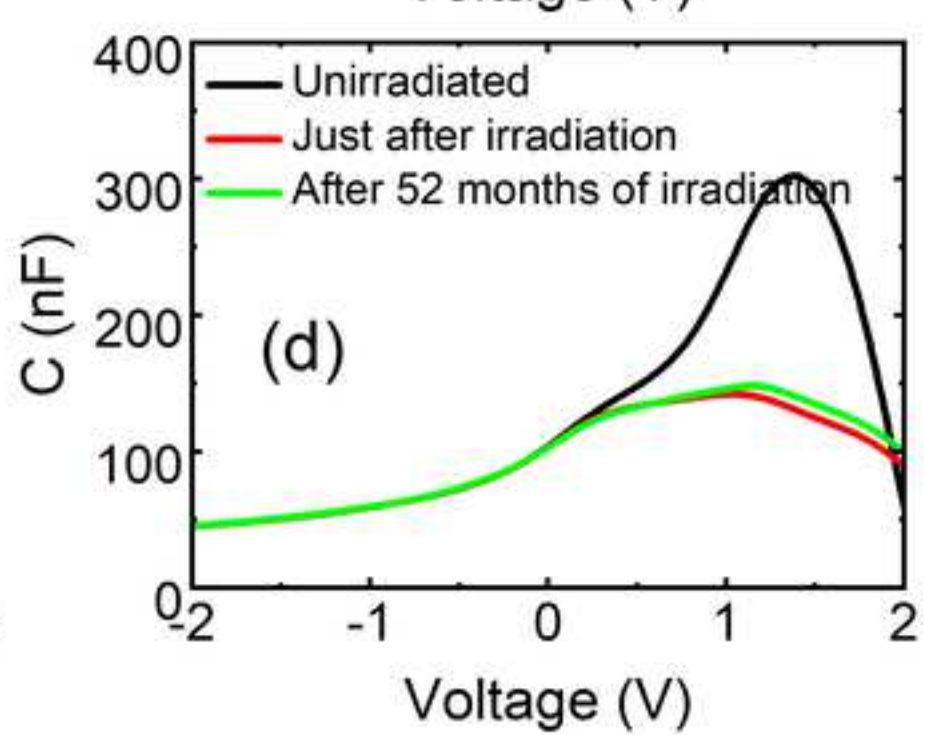
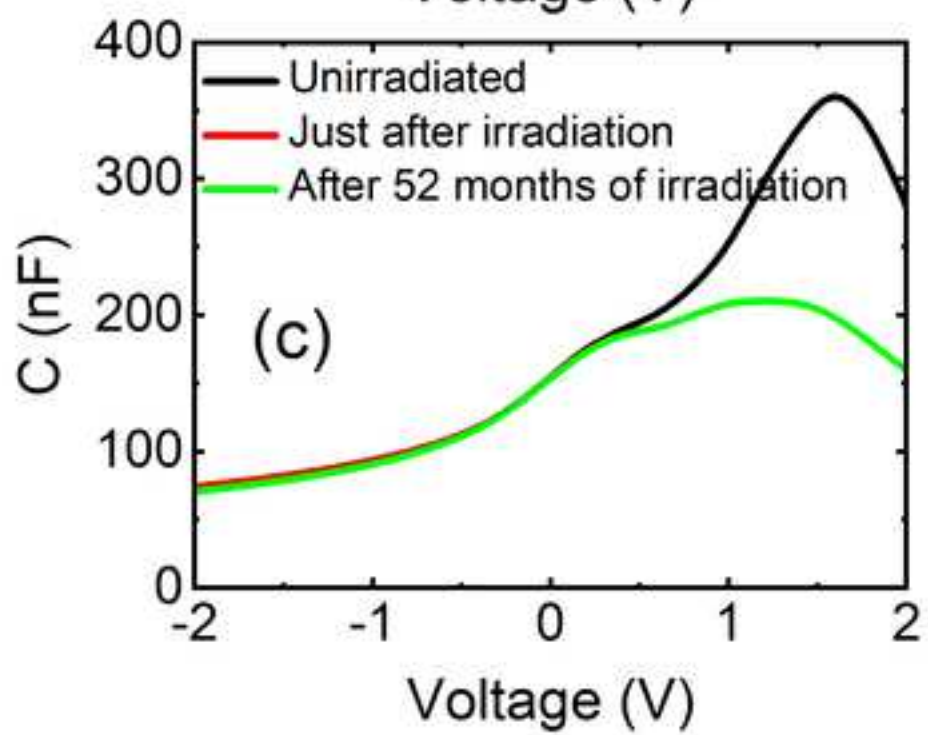
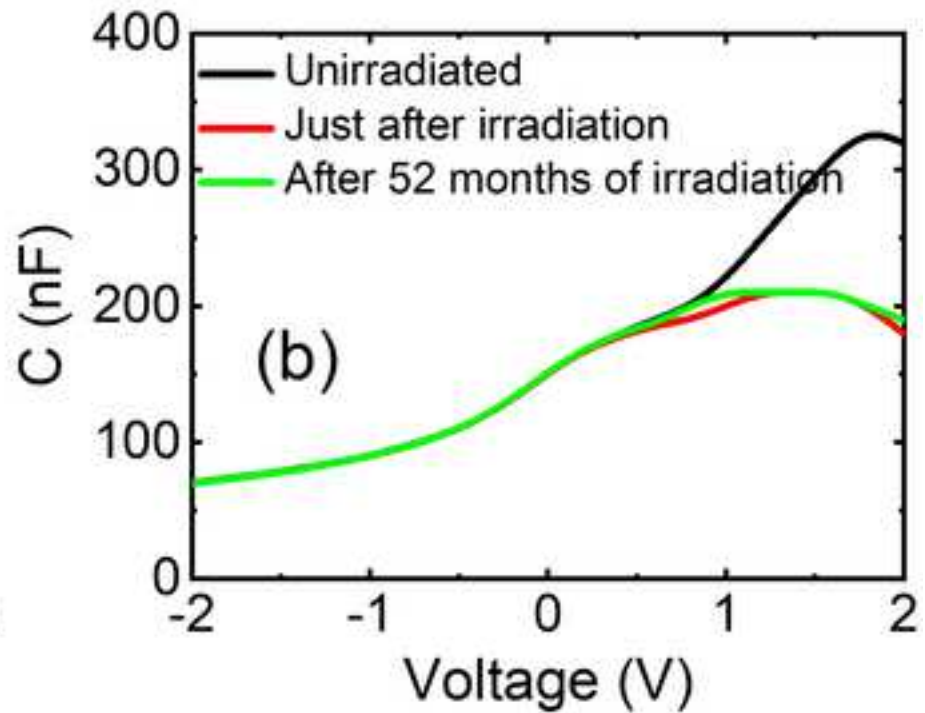
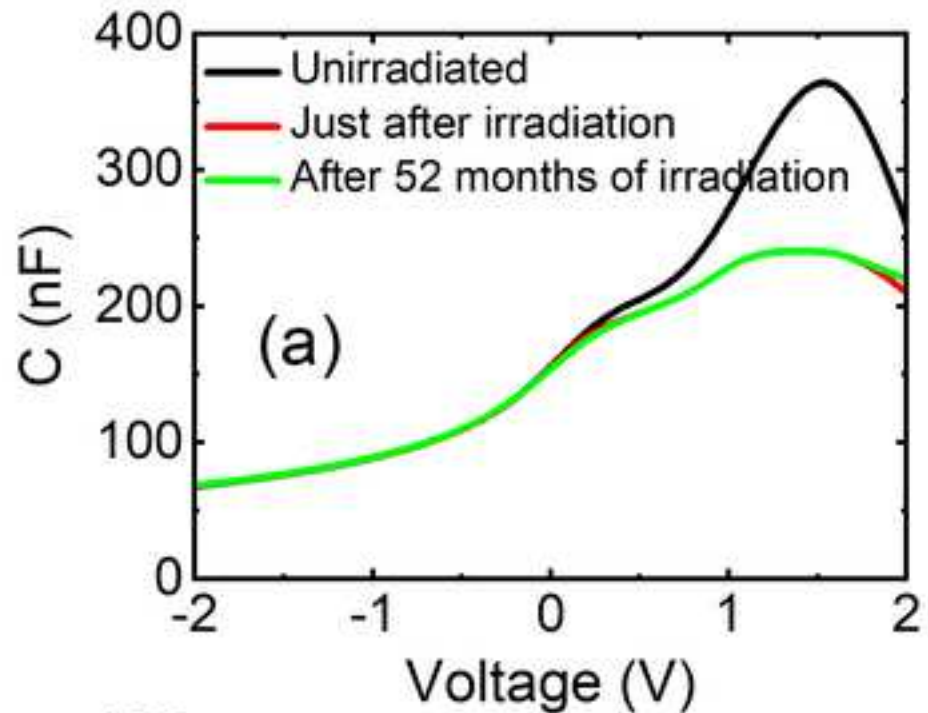
[Click here to access/download;Figure;Figure 9.jpg](#)

Figure 10

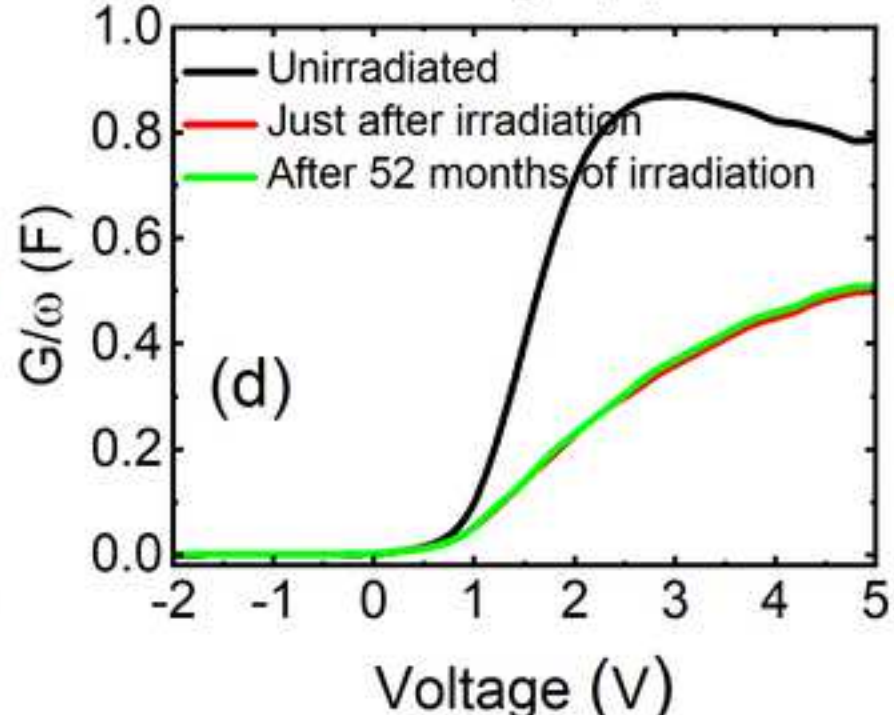
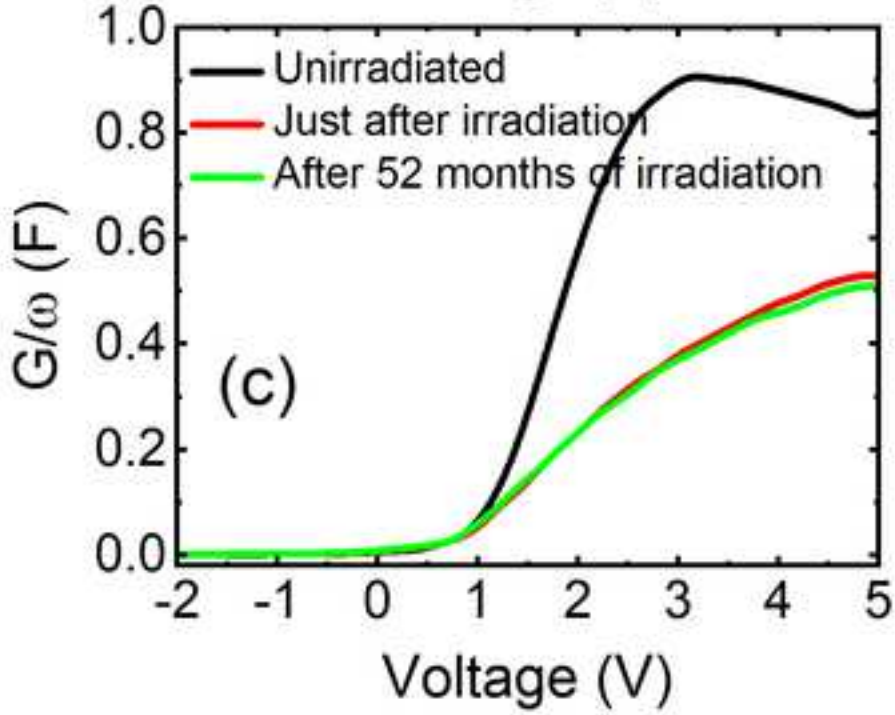
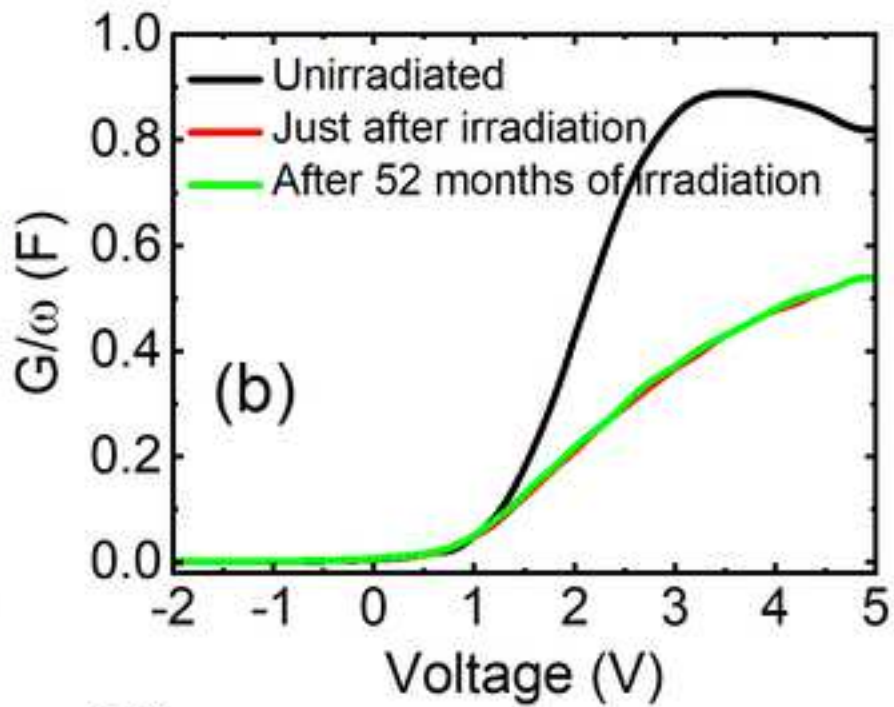
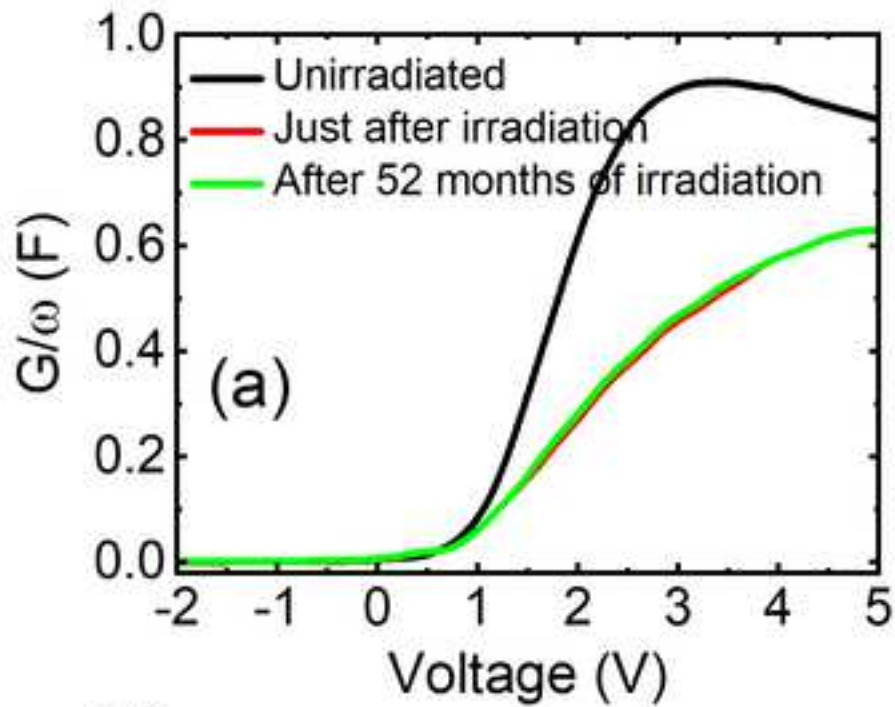
[Click here to access/download;Figure;Figure 10.jpg](#)

Table 1. Calculated diode ideality factors of the cells.

	225 Gy	450 Gy	675 Gy	900 Gy
Unirradiated	1.71	1.67	1.62	1.76
Just after Irradiation	1.86	1.94	2.18	2.43
After 52 months of irradiation	1.74	2.08	1.95	2.13

Table 2. Basic cell parameters obtained from illuminated I-V given in Fig.3

Dose (Gy)	Unirradiated				Just after irradiation				After 52 months of irradiation			
	Voc (mV)	Jsc (mA/ cm ²)	FF (%)	η (%)	Voc (mV)	Jsc (mA/ cm ²)	FF (%)	η (%)	Voc (mV)	Jsc (mA/ cm ²)	FF (%)	η (%)
225	578	36.7	77.1	16.3	553	31.9	78.7	13.9	558	34.4	62.9	12.1
450	586	35.6	74.9	15.6	542	29.3	76.5	12.1	546	31.2	63.7	10.8
675	580	35.8	76.5	15.9	538	28.8	76.7	11.9	540	30.4	69.5	11.4
900	585	34.6	77.8	15.7	534	26.9	78.4	11.3	537	27.9	73.4	10.9

Table 3. Calculated loss and recovery in J_{SC} values from illuminated I-V measurements (Fig. 2) for different radiation doses. J_{SC0} , J_{SC1} and J_{SC2} are the short circuit current densities of the cells before irradiation, just after irradiation and after a 52-month period of irradiation respectively.

Dose (Gy)	Loss in J_{SC} ($J_{SC0} - J_{SC1}$) (mA/cm ²)	Recovery in J_{SC} ($J_{SC2} - J_{SC1}$) (mA/cm ²)	Percentage in J_{SC} recovery (%)
225	4.70	2.47	52.6
450	6.37	1.92	30.1
675	6.97	1.62	23.2
900	7.60	1.23	16.2

Table 4. Calculated loss and recovery in J_{SC} values from EQE measurements (Fig. 5) for different radiation doses. J_{SC0} , J_{SC1} and J_{SC2} are the short circuit current densities of the cells for unirradiated, just irradiated and after 52 months of irradiation cases respectively.

Dose (Gy)	Loss in J_{SC} ($J_{SC0} - J_{SC1}$) (mA/cm ²)	Recovery in J_{SC} ($J_{SC2} - J_{SC1}$) (mA/cm ²)	Percentage in J_{SC} recovery (%)
225	2.75	2.24	81.5
450	4.62	1.73	37.4
675	5.36	1.89	35.3
900	5.87	2.60	44.3

Table 5. Percentage of loss and recovery in the diffusion length of electrons calculated at 800 and 900 nm.

Dose (Gy)	Percentage in Ln Loss (%)	Percentage in Ln Recovery (%)	Percentage in Ln Loss (%)	Percentage in Ln Recovery (%)
	800 nm		900 nm	
225	48	66	65	36
450	61	36	80	21
675	72	30	82	17
900	71	49	83	28